Self-assembly of Taper-shaped Monoesters of Oligo(ethylene Oxide) with 3,4,5-Tris(*n*-dodecan-1-yloxy)benzoic Acid and of their Polymethacrylates into Tubular Supramolecular Architectures Displaying a Columnar Hexagonal Mesophase

Virgil Percec,*,[a] Dimitris Tomazos,[a] James Heck,[a] Helen Blackwell[a] and Goran Ungar[b]
[a] *Department of Macromolecular Science, Case Western Reserve University, Cleveland, OH 44106-2699, USA*
[b] *Department of Engineering Materials and Centre for Molecular Materials, The University of Sheffield, Sheffield, UK S1 3DU*

The synthesis of the monoesters of oligo(ethylene oxide) and octane-1,8-diol with 3,4,5-tris(*n*-alkan-1-yloxy)benzoic acids and of their corresponding polymethacrylates is described. The $LiCF_3SO_3$ complexes of the monoesters of triethylene glycol with 3,4,5-tris(*n*-dodecan-1-yloxy)-benzoic acid (**3-12-3**), and with 3,4,5-tris(*n*-octadecan-1-yloxy)benzoic acid (**3-18-3**), as well as the polymethacrylates of the monoesters of mono-(**5-12-1**), di-(**5-12-2**), tri-(**5-12-3**) and tetra-(**5-12-4**) ethylene glycol with 3,4,5-tris(*n*-dodecan-1-yloxy)benzoic acid self-assemble into a cylindrical supramolecular architecture which displays a columnar hexagonal (Φ_h) mesophase. This cylindrical supramolecular architecture was characterized by a combination of techniques including differential scanning calorimetry, wide- and small-angle X-ray scattering, thermal optical polarized microscopy, and molecular modelling. The characterization results suggest a model that resembles the cylindrical architecture that forms by the self-assembly of low molar mass and polymerized inverse micelles. A cross-section of the cylindrical assembly is constituted of about five molecules of **3-12-3** in its $LiCF_3SO_3$ complex or about four to five repeats units of **5-12-*n*** with their oligooxyethylenic segments melted and segregated in the inner core of the cylinder and their melted alkyl tails radiating towards the periphery of the cylinder. The driving force for the cylindrical self-assembly is provided by a fine balance of exo- and endo-recognition processes. Exo-recognition is the result of the tapered shape and hydrophobic character of the 3,4,5-tris(*n*-dodecan-1-yloxy)benzoate group. Endo-recognition is generated by either the combination of dipolar and ionic interactions of the oligo(ethylene oxide) receptor ($LiCF_3SO_3$ complex of **3-12-3**) or the combination of dipolar interactions and covalent bonding (**5-12-*n***). The necessity of the presence of endo-recognition for the self-assembly of the cylindrical supramolecular architecture is demonstrated by the replacement of the oligo(ethylene oxide) receptor by a non-polar aliphatic spacer. Comparison between the 'molecular' polymethacrylate backbone (in **5-12-3**) and the 'supramolecular polymer backbone' (formed *via* ionic interactions in the complex of **3-12-3**) indicates that in this particular example, the ionic interactions generated by the dissolved ion-pairs stabilize the supramolecular assembly to a greater extent than does the covalent bonding.

Current research in our laboratory has applied the principles of self-assembly of biological systems to the generation of synthetic cylindrically shaped supramolecular architectures.[1-3] The basic synthetic approach used was inspired by the self-assembly of Tobacco Mosaic Virus (TMV)[4] and of cylindrical micelles[5a-e] which generate cylindrical supramolecular architectures by a combination of endo- and exo-recognition processes.[4] In the case of TMV the tapered shape of the constituent proteins[1,4] while in the case of cylindrical micelles the truncated cone shape of lipids or other amphiphilic molecules[5a] are responsible for the exo-recognition process. TMV is the most challenging system since its taper-shaped proteins can self-assemble either in the presence of a single chain of RNA, or in its absence, by changing the pH of the aqueous solution of the proteins.[4] Therefore, in this case the endo-recognition process takes place either between RNA and proteins or only in-between proteins. A more detailed discussion of this self-assembly process has been presented elsewhere.[1]

In our first series of investigations, exo-recognition was provided by the tapered shape and hydrophobic interactions of 3,4,5-tris[*p*-(*n*-dodecan-1-yloxy)benzyloxy]benzoyl (DOBOB) group [Scheme 1(*a*, *b*)].[1-3] Various examples of low molar mass liquid crystals based on DOBOB have been reviewed.[6] In our first synthetic approach,[1] the endo-recognition process was replaced by covalent bonding generated by a living cationic polymerization. The polymerization reaction produces oligomers of different degrees of polymerization (DP). The oligomers with the appropriate DP selectively self-assemble into the cylindrical supramolecular architecture.[1] The replacement of the endo-recognition process by a polymerization reaction allowed the fast selection of the most suitable tapered group which can function as an exo-receptor. In a subsequent synthetic approach, we used the benzo-15-crown-5 endo-receptor to provide the endo-recognition process.[2] While 4'-methyl(benzo-15-crown-5)-3,4,5-tris[4-(*n*-dodecan-1-yloxy)-benzyloxy]benzoate forms a lamellar crystal structure, the complexation of its benzo-15-crown-5 endo-receptor with $NaCF_3SO_3$ or KCF_3SO_3 destabilizes its crystalline phase and induces its self-assembly into a cylindrical architecture which displays an enantiotropic columnar hexagonal (Φ_h) mesophase.[2] In a more recent experiment,[3] we have substituted the benzo-15-crown-5 endo-receptor with non-selective hydroxy-terminated oligo(ethylene oxide) endo-receptors. In this case, endo-recognition was effected *via* the hydrogen

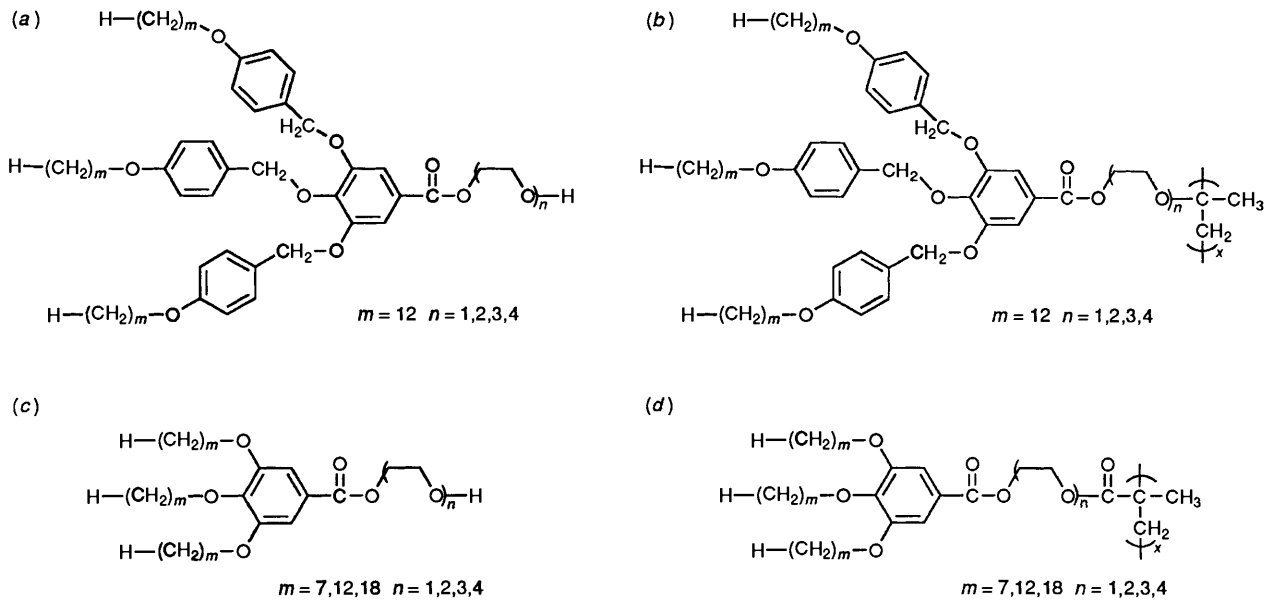

Scheme 1 (*a*) Low molar mass tapers based on the monoesters of oligo(oxyethylene oxide) and the 3,4,5-tris[4-(*n*-dodecan-1-yloxy)-benzyloxy]benzoate tapered group; (*b*) the corresponding polymethacrylates; (*c*) low molar mass tapers based on the monoesters of oligo-(oxyethylene oxide) and the narrower 3,4,5-tris(alkan-1-yloxy)benzoic acid; (*d*) the corresponding polymethacrylates

bonding and dipolar interactions of the oligo(ethylene oxide) receptor, and ultimately *via* ionic interactions generated by alkali-metal complexation. These last low molar mass compounds also self-assemble into cylindrical supramolecular architectures that display an enantiotropic Φ_h phase. The synthesis of their corresponding polymethacrylates led to the first direct comparison of a 'molecular' polymer backbone with a 'supramolecular polymer backbone'.[3]

The goal of this paper is to present a synthetically simpler approach to the design of cylindrical supramolecular architectures that utilizes concepts closer to those in the self-assembly of inverse micelles except that the present systems self-assemble in the melt phase. The synthesis, structure and phase behaviour of monoesters of non-selective oligo(ethylene oxide) endo-receptors with 3,4,5-tris(*n*-alkan-1-yloxy)benzoic acid [Scheme 1(*c*, *d*)] and of their corresponding polymethacrylates is described. The ability of the oligo(ethylene oxide) endo-receptor to function by a combination of dipolar interactions and non-selective complexation of metal salts will be demonstrated and compared with that generated *via* the molecular polymethacrylate backbone. The exo-receptor 3,4,5-tris(*n*-alkan-1-yloxy)-benzoate lacks the benzyloxy groups present in the 3,4,5-tris[*p*-(*n*-alkan-1-yloxy)benzyloxy]benzoate unit used previously,[1-3] which made the last one resemble a fragment of disc-like shape.[1-3]

Experimental

Materials.—Tetraethylene glycol (99%), triethylene glycol (99%), tetrabutylammonium hydrogen sulfate (TBAH, 97%), toluenesulfonyl chloride (TsCl, 98%), 1-bromooctadecane (96%), propyl gallate (98%), octane-1,8-diol (98%) (all from Aldrich), 1-bromoheptane (99%, Fluka), 4-dimethylamino-pyridine (DMAP, 98%, Fluka), methacryloyl chloride (97%, Fluka), ethylene glycol (Fisher), diethylene glycol (Pfaltz & Bauer), and the other conventional reagents were used as received. Tetrahydrofuran (THF) was distilled from $LiAlH_4$. Triethylamine (Et_3N) was heated overnight at 60 °C over KOH, distilled from KOH, and then stored over KOH. Benzene was washed with 50 cm^3 portions of H_2SO_4 until they remained relatively uncoloured, washed with water to neutral pH, dried over $MgSO_4$, filtered, heated at 80 °C overnight over $LiAlH_4$, and then was distilled. $LiCF_2SO_3$ (97%, Aldrich) was dried at 120 °C under vacuum for 24 h. Azoisobutyronitrile (AIBN, Fluka) was recrystallized from MeOH below 40 °C.

Techniques.—^1H NMR (200 MHz) spectra were recorded on a Varian XL-200 spectrometer, at 20 °C using Me_4Si as an internal standard. Infrared (IR) spectra were recorded on a Perkin-Elmer 1320 infrared spectrometer. Relative molecular weights of polymers were measured by gel permeation chromatography (GPC) with a Perkin-Elmer Series 10 LC instrument equipped with an LC-100 column oven and a Nelson 900 series integrator data station. A set of two Polymer Laboratories PL gel columns of 5×10^2 and 10^4 Å and $CHCl_3$ as solvent (1 cm^3 min^{-1}) were used. The measurements were made at 40 °C using a UV detector. Polystyrene standards were used for the calibration plot. High pressure liquid chromatography (HPLC) experiments were performed with the same instrument. Perkin-Elmer DSC-4 and DSC-7 differential scanning calorimeters were used to determine the thermal transitions which were reported as the maximum and minimum of their endothermic and exothermic peaks. In all cases, heating and cooling rates were 20 °C min^{-1} unless specified. Glass transition temperatures (T_g) were read at the middle of the change in heat capacity. First heating scans differ from second and subsequent heating scans. However, second and subsequent heating scans are identical. The difference between various DSC scans will be discussed. X-Ray scattering patterns were recorded using either a helium-filled flat plate wide angle (WAXS) camera or a pinhole-collimated small angle (SAXS) camera. Ni-filtered Cu-Kα radiation was used. The samples were in the form of (*a*) as prepared polymers in the form of a powder or (*b*) bulk samples in Lindemann thin-wall 1 mm capillaries cooled from the melt. The temperature stability of the X-ray heating cell was ±0.1 °C. A Carl-Zeiss optical polarized microscope (magnification × 100) equipped with a Mettler FP82 hot stage and a Mettler FP80 central processor was used to observe the thermal transitions and to analyse the anisotropic textures. Molecular modelling was done using CSC Chem3D™ from Cambridge Scientific Computing, Inc.

Synthesis of Monomers and Polymers.—**1-7**, **1-12** and **1-18** were synthesized by the alkylation of propyl gallate followed

by hydrolysis and neutralization as reported previously for the synthesis of **1-12**.[7] Analytical data for **1-12** have already been reported.[7]

3,4,5-*Tris*(n-*heptan*-1-*yloxy*)*benzoic acid* (**1-7**). From 15.3 g (72 mmol) propyl gallate and 40 g (220 mmol) of 1-bromoheptane were obtained 31.0 g (92%) of white solid **1-7**. Purity: 99% (HPLC). M.p. 40–41 °C δ($CDCl_3$) 0.85 (t, 9 H, CH_3), 1.27, 1.42 (overlapped peaks, 24 H, CH_2s), 1.77 (m, 6 H, CH_2CH_2O), 3.96 (overlapped t, 6 H, CH_2O), 7.27 (s, 2 H, ArH); ν_{max}/cm^{-1} 1670 (C=O).

3,4,5-*Tris*(n-*octadecan*-1-*yloxy*)*benzoic acid* (**1-18**). From 8.2 g (39 mmol) propyl gallate and 40 g (120 mmol) of 1-bromooctadecane were obtained 20.1 g (56%) of white solid **1-18**. Purity: 99% (HPLC). M.p. 83–85 °C δ($CDCl_3$) 0.85 (t, 9 H, CH_3), 1.22, 1.43 (overlapped peaks, 90 H, CH_2s), 1.76 (m, 6 H, CH_2CH_2O), 3.97 (overlapped t, 6 H, CH_2O), 7.26 (s, 2 H, ArH); ν_{max}/cm^{-1} 1675 (C=O).

2-[2-(2-*Hydroxyethoxy*)*ethoxy*]*ethyl* 3,4,5-*Tris*(n-*heptan*-1-*yloxy*)*benzoate* (**3-7-3**).—Compounds **3-7-3**, **3-12-*n***, **3-18-3** and **3-12-*p*** were synthesized using the same procedure as described below. An example is given here. In a flask were placed 6.00 g (12.9 mmol) of **1-7**, 15.50 g (103.0 mmol) of triethylene glycol (**2-3**), 2.40 g (12.6 mmol) of TsCl, 0.50 g (4.0 mmol) of DMAP, 0.50 g (2.0 mmol) of TBAH, 7.2 g (52.0 mmol) of anhydrous K_2CO_3 and 50 cm^3 of dry THF. The flask was sealed with a stopper and heated with stirring at 45 °C for 16 h. The reaction mixture was allowed to cool to room temperature and was then poured into 1000 cm^3 of H_2O. CH_2Cl_2 (150 cm^3) was then added. The reaction mixture was slowly acidified with dilute HCl with vigorous stirring until pH 1 was reached. The organic layer was separated, washed four additional times with 600 cm^3 of H_2O, and then dried over $MgSO_4$. The mixture was filtered to remove the solid $MgSO_4$ and then evaporated. The product was then purified by column chromatography (silica gel, $CHCl_3$ eluent) and the solvent was evaporated off to yield 3.80 g (49.4%) of clear liquid **3-7-3**. Purity: 98% (HPLC). δ($CDCl_3$) 0.89 (t, 9 H, CH_3), 1.31 [overlapped peaks, 24 H, $(CH_2)_4$], 1.79 (overlapped peaks, 6 H, CH_2CH_2OPh), 2.55 (br, 1 H, OH), 3.61 (t, 2 H, CH_2OH, *J* 4.6), 3.70 (s, 6 H, $CH_2CH_2OCH_2CH_2OH$), 3.84 (t, 2 H, $COOCH_2$-CH_2, *J* 4.6 Hz), 4.02 (overlapped peaks, 6 H, CH_2OPh), 4.48 (t, 2 H, $COOCH_2$, *J* 4.8), 7.29 (s, 2 H, Ar*H*COO–); ν_{max}/cm^{-1} 3200–3600 (OH), 1710 (C=O).

2-*Hydroxyethyl* 3,4,5-*tris*(n-*dodecan*-1-*yloxy*)*benzoate* (**3-12-1**). From 9.01 g (13.3 mmol) of **1-12**, 5.79 g (93.2 mmol) of ethylene glycol (**2-1**), 2.46 g (12.9 mmol) of TsCl, 0.20 g (1.64 mmol) of DMAP, 0.20 g (0.59 mmol) of TBAH and 5.52 g (40.0 mmol) of anhydrous K_2CO_3 were obtained 3.12 g (32%) of a white solid **3-12-1**. Purity: 99% (HPLC). M.p. 44–45 °C, δ($CDCl_3$) 0.85 (t, 9 H, CH_3), 1.27 [overlapped peaks, 54 H, $(CH_2)_9$], 1.75 (overlapped peaks, 6 H, CH_2CH_2OPh), 3.96 (overlapped peaks, 8 H, CH_2CH_2OPh and CH_2OH), 4.46 (t, 2 H, CH_2OOC, *J* 4.3 Hz), 7.25 (s, 2 H, Ar*H*COO); ν_{max}/cm^{-1} 3200–3600 (OH), 1705 (C=O).

2-(2-*Hydroxyethoxy*)*ethyl* 3,4,5-*tris*(n-*dodecan*-1-*yloxy*)*benzoate* (**3-12-2**). From 10.0 g (14.8 mmol) of **1-12**, 11.0 g (103 mmol) of diethylene glycol (**2-2**), 2.74 g (14.4 mmol) of TsCl, 0.20 g (1.64 mmol) of DMAP, 0.20 (0.59 mmol) of TBAH, and 6.13 g (44.4 mmol) of K_2CO_3 were obtained 2.65 g (23%) of white solid **3-12-2**. Purity: 99% (HPLC). M.p. 42–43 °C, δ($CDCl_3$) 0.86 (t, 9 H, CH_3), 1.27 [overlapped peaks, 54 H, $(CH_2)_9$], 1.75 (overlapped peaks, 6 H, CH_2CH_2OPh), 3.65 (t, 2 H, CH_2OH, *J* 5.0), 3.75 (t, 2 H, CH_2CH_2OH, *J* 5.0), 3.83 (t, 2 H, CH_2CH_2OOC, *J* 5.0), 4.01, (t, 6 H, CH_2CH_2OPh, *J* 6.0), 4.47 (t, 2 H, CH_2OOC, *J* 5.0), 7.24 (s, 2 H, ArHCOO); ν_{max}/cm^{-1} 3200–3600 (OH), 1705 (C=O).

2-[2-(2-*Hydroxyethoxy*)*ethoxy*]*ethyl* 3,4,5-*tris*(n-*dodecan*-1-*yloxy*)*benzoate* (**3-12-3**). From 6.00 g (8.90 mmol) of **1-12**, 9.36 g (62.3 mmol) of triethylene glycol (**2-3**), 1.66 g (8.70 mmol) of TsCl, 0.20 g (1.64 mmol) of DMAP, 0.20 g (0.59 mmol) of TBAH, and 5.30 g (38.0 mmol) of K_2CO_3 were obtained 4.20 g (58%) of a white solid **3-12-3**. Purity: 99% (HPLC). M.p. 47–48 °C, *d* = 1.02 g cm^{-3} (20 °C); δ($CDCl_3$) 0.88 (t, 9 H, CH_3), 1.27 [overlapped peaks, 54 H, $(CH_2)_9$], 1.78 (overlapped peaks, 6 H, CH_2CH_2OPh), 3.63 (t, 2 H, CH_2OH, *J* 4.7), 3.70 (s, 6 H, $CH_2CH_2OCH_2CH_2OH$), 3.84 (t, 2 H, $COOCH_2CH_2$, *J* 4.5), 4.02 (t, 6 H, CH_2CH_2OPh, *J* 6.1), 4.48 (t, 2 H, $COOCH_2$, *J* 4.7), 7.29 (s, 2 H, ArHCOO); ν_{max}/cm^{-1} 3200–3600 (OH), 1700 (C=O).

2-{2-[2-(2-*Hydroxyethoxy*)*ethoxy*]*ethoxy*}*ethyl* 3,4,5-*tris*(n-*dodecan*-1-*yloxy*)*benzoate* (**3-12-4**). From 7.00 g (10.4 mmol) of **1-12**, 14.10 g (61.9 mmol) of tetraethylene glycol (**2-4**), 1.92 g (10.0 mmol) of TsCl, 0.20 g (1.64 mmol) of DMAP, 0.20 g (0.59 mmol) of TBAH, and 4.29 g (31.1 mmol) of K_2CO_3 were obtained 2.33 g (26%) of a clear liquid **3-12-4**. Purity: 99% (HPLC), δ($CDCl_3$) 0.84 (t, 9 H, CH_3), 1.28 [overlapped peaks, 54 H, $(CH_2)_9$], 1.78 (overlapped peaks, 6 H, CH_2CH_2OPh), 3.60 (t, 2 H, CH_2OH, *J* 5.9), 3.73, 3.77 (2 overlapped singlets, 10 H, OCH_2CH_2O), 3.83 (t, 2 H, $COOCH_2CH_2$, *J* 5.0), 4.01 (t, 6 H, CH_2CH_2OPh, *J* 6.7), 4.47 (t, 2 H, $COOCH_2$, *J* 5.9), 7.24 (s, 2 H, Ar*H*COO); ν_{max}/cm^{-1} 3200–3600 (OH), 1715 (C=O).

8-*Hydroxyoctyl* 3,4,5-*tris*(n-*dodecan*-1-*yloxy*)*benzoate* (**3-12-*p***). From 5.00 g (7.40 mmol) of **1-12**, 7.00 g (47.9 mmol) of octane-1,8-diol (**2-p**), 1.41 g (7.40 mmol) of TsCl, 0.20 g (1.64 mmol) of DMAP, 0.20 g (0.59 mmol) of TBAH, and 5.00 g (36.2 mmol) of K_2CO_3 were obtained 3.42 g (56%) of white solid **3-12-*p***. Purity: 99% (HPLC), m.p. 44–45 °C; δ($CDCl_3$) 0.88 (t, 9 H, CH_3), 1.27 [overlapped peaks, 64 H, (CH_2)], 1.80 (overlapped peaks, 8 H, CH_2CH_2OPh and $COOCH_2CH_2$), 3.65 (t, 2 H, CH_2OH, *J* 6.3), 4.02 (t, 6 H, CH_2CH_2OPh, *J* 6.5), 4.29 (t, 2 H, $COOCH_2$, *J* 6.8), 7.26 (s, 2 H, ArHCOO); ν_{max}/cm^{-1} 3200–3600 (OH), 1710 (C=O).

2-[2-(2-*Hydroxyethoxy*)*ethoxy*]*ethyl* 3,4,5-*tris*(n-*octadecan*-1-*yloxy*)*benzoate* (**3-18-3**). From 5.40 g (5.1 mmol) of **1-18**, 7.66 g (51.0 mmol) of triethylene glycol (**2-3**), 0.95 g (5.0 mmol) of TsCl, 0.20 g (1.6 mmol) of DMAP, 0.20 g (0.8 mmol) of TBAH, 3.0 g (22.0 mmol) of K_2CO_3 were obtained 3.10 g (57.4%) of a white solid **3-18-3**. Purity: 99% (HPLC), m.p. 68–69 °C (DSC at 20 °C min^{-1}); δ($CDCl_3$) 0.88 (t, 9 H, CH_3), 1.26 [overlapped peaks, 90 H, $(CH_2)_{15}$], 1.78 (overlapped peaks, 6 H, CH_2CH_2OPh), 2.35 (br, 1 H, OH), 3.61 (t, 2 H, CH_2OH, *J* 4.7), 3.70 (s, 6 H, $CH_2CH_2OCH_2CH_2OH$), 3.81 (t, 2 H, $COOCH_2CH_2$, *J* 4.6), 4.01 (overlapped peaks, 6 H, CH_2CH_2OPh), 4.48 (t, 2 H, $COOCH_2$, *J* 4.8 Hz), 7.29 (s, 2 H, ArHCOO); ν_{max}/cm^{-1} 3200–3600 (OH), 1700 (C=O).

2-[2-(2-*Methacryloyloxyethoxy*)*ethoxy*]*ethyl* 3,4,5-*Tris*(n-*heptan*-1-*yloxy*)*benzoate* (**4-7-3**).—Compounds **4-7-3**, **4-12-*n***, **4-18-3** and **4-12-*p*** were synthesized using the same procedure. An example is given here. In a 100 cm^3 round-bottomed flask equipped with $CaSO_4$ drying tube were placed 3.70 g (6.2 mmol) of **3-7-3** and 2.40 cm^3 (24.8 mmol) of methacryloyl chloride in 20 cm^3 dry CH_2Cl_2 and the mixture was cooled to 0–5 °C with an ice–water bath. Dry Et_3N (4.84 cm^3, 34.7 mmol) was added dropwise and the reaction mixture was stirred at this temperature for 1 h. The reaction mixture was poured into water and extracted with 100 cm^3 of CH_2Cl_2. The organic layer was separated, washed several times with 5% aqueous HCl, water and finally dried over anhydrous $MgSO_4$. The solvent was removed on a rotary evaporator at room temperature to yield a viscous oil. The crude product was then purified by column chromatography (neutral alumina, THF) to yield 2.80 g (67.9%) of a clear liquid **4-7-3**. Purity: 99% (HPLC), δ($CDCl_3$) 0.89 (t, 9 H, CH_3), 1.31 [overlapped peaks, 24 H, $(CH_2)_4$], 1.78 (overlapped peaks, 6 H, CH_2CH_2OPh), 1.94 (s,

3 H, $CH_3C{=}CH_2$), 3.70–3.75 [overlapped peaks, 6 H, $CH_2CH_2OCH_2CH_2OOCC(CH_3){=}CH_2$], 3.83 (t, 2 H, PhCOOCH$_2CH_2$, *J* 4.9), 4.01 (overlapped peaks, 6 H, CH_2CH_2OPh), 4.30 (t, 2 H, $CH_2OOCCCH_3$, *J* 5.0), 4.46 (t, 2 H, COOCH$_2$, *J* 5.3), 5.56 [s, 1 H, C(CH$_3$)=CH_2 *trans* to C=O], 6.13 [s, 1 H, C(CH$_3$)=CH_2 *cis* to C=O], 7.27 (s, 2 H, ArHCOO); ν_{max}/cm^{-1} 1710 (C=O).

2-*Methacryloyloxyethyl* 3,4,5-*tris*(n-*dodecan*-1-*yloxy*)*benzoate* (**4-12-1**). From 2.20 g (3.06 mmol) of **3-12-1**, 1.20 cm^3 (12.2 mmol) of methacryloyl chloride, and 2.38 cm^3 (17.1 mmol) of Et_3N, were obtained 1.72 g (71.5%) of white solid **4-12-1**. Purity: 99% (HPLC), m.p. 48 °C (DSC at 20 °C min^{-1}); δ($CDCl_3$) 0.88 (t, 9 H, CH_3), 1.26 [overlapped peaks, 54 H, $(CH_2)_9$], 1.76 (overlapped peaks, 6 H, CH_2CH_2OPh), 1.95 (s, 3 H, $CH_3C{=}CH_2$), 4.00 (overlapped peaks, 6 H, CH_2CH_2OPh), 4.52 (overlapped peaks, 4 H, COOCH_2CH_2), 5.59 [s, 1 H, C(CH$_3$)=CH_2 *trans* to C=O], 6.15 [s, 1 H, C(CH$_3$)=CH_2 *cis* to C=O), 7.26 (s, 2 H, ArHCOO); ν_{max}/cm^{-1} 1715 (C=O).

2-(2-*Methacryloyloxyethoxy*)*ethyl* 3,4,5-*tris*(n-*dodecan*-1-*yloxy*)*benzoate* (**4-12-2**). From 2.0 g (2.62 mmol) of **3-12-2**, 1.01 cm^3 (10.5 mmol) of methacryloyl chloride, and 2.05 cm^3 (14.7 mmol) of Et_3N were obtained 0.91 g (41.8%) of a white solid **4-12-2**. Purity: 99% (HPLC), m.p. 42 °C (DSC at 20 °C min^{-1}); δ($CDCl_3$) 0.88 (t, 9 H, CH_3), 1.27 [overlapped peaks, 54 H, $(CH_2)_9$], 1.78 (overlapped peaks, 6 H, CH_2CH_2OPh), 1.92 (s, 3 H, $CH_3C{=}CH_2$), 3.81 (overlapped peaks, 4 H, $CH_2CH_2OCH_2CH_2OOCCCH_3$), 4.01 (overlapped peaks, 6 H, CH_2CH_2OPh), 4.32 (t, 2 H, $CH_2OOCCCH_3$, *J* 5.0), 4.47 (t, 2 H, COOCH_2, *J* 5.1), 5.55 [s, 1 H, C(CH$_3$)=CH_2 *trans* to C=O)], 6.11 [s, 1 H, C(CH$_3$)=CH_2 *cis* to C=O], 7.27 (s, 2 H, ArHCOO); ν_{max}/cm^{-1} 1710 (C=O).

2-[2-(2-*Methacryloyloxyethoxy*)*ethoxy*]*ethyl* 3,4,5-*tris*(n-*dodecan*-1-*yloxy*)*benzoate* (**4-12-3**). From 1.10 g (1.36 mmol) of **3-12-3**, 0.53 cm^3 (5.44 mmol) of methacryloyl chloride and 1.06 cm^3 (7.62 mmol) of Et_3N, were obtained 0.93 g (78.2%) of white **4-12-3**. Purity: 99% (HPLC), m.p. 37 °C (DSC at 20 °C min^{-1}); δ($CDCl_3$) 0.88 (t, 9 H, CH_3), 1.27 [overlapped peaks, 54 H, $(CH_2)_9$], 1.81 (overlapped peaks, 6 H, CH_2CH_2OPh), 1.94 (s, 3 H, $CH_3C{=}CH_2$), 3.69–3.74 (overlapped peaks, 6 H, $CH_2CH_2OCH_2CH_2OOC$-CCH_3), 3.83 (t, 2 H, PhCOOCH$_2$-CH_2, *J* 5.0), 4.01 (overlapped peaks, 6 H, CH_2CH_2OPh), 4.30 (t, 2 H, $CH_2OOCCCH_3$, *J* 5.2), 4.46 (t, 2 H, COOCH_2, *J* 4.8), 5.57 (s, 1 H, C(CH$_3$)=CH_2 *trans* to C=O), 6.13 [s, 1 H, C(CH$_3$)=CH_2 *cis* to C=O], 7.27 (s, 2 H, ArHCOO); ν_{max}/cm^{-1} 1715 (C=O).

2-{2-[2-(2-*Methacryloyloxyethoxy*)*ethoxy*]*ethoxy*}*ethyl*-3,4,5-*tris*(n-*dodecan*-1-*yloxy*)*benzoate* (**4-12-4**). From 4.00 g (4.7 mmol) of **3-12-4**, 1.80 cm^3 (18.8 mmol) of methacryloyl chloride and 3.70 cm^3 (26.3 mmol) of Et_3N were obtained 3.10 g (71.8%) of a clear liquid **4-12-4**. Purity: 99% (HPLC), δ($CDCl_3$) 0.88 (t, 9 H, CH_3), 1.27 [overlapped peaks, 54 H, $(CH_2)_9$], 1.77 (overlapped peaks, 6 H, CH_2CH_2OPh), 1.94 (s, 3 H, $CH_3C{=}CH_2$), 3.66–3.73 [overlapped peaks, 10 H, $(CH_2CH_2O)_2CH_2CH_2OOCC(CH_3)$], 3.82 (t, 2 H, PhCOOCH$_2CH_2$, *J* 4.6), 4.01 (overlapped peaks, 6 H, CH_2CH_2OPh), 4.30 (t, 2 H, $CH_2OOCCCH_3$, *J* 4.8), 4.46 (t, 2 H, COOCH$_2$, *J* 5.2), 5.57 [s, 1 H, C(CH$_3$)=CH_2 *trans* to C=O], 6.13 [s, 1 H, C(CH$_3$)=CH_2 *cis* to C=O], 7.27 (s, 2 H, ArHCCO); ν_{max}/cm^{-1} 1715 (C=O).

8-*Methacryloyloxyoctyl* 3,4,5-*tris*(n-*dodecan*-1-*yloxy*)*benzoate* (**4-12-*p***). From 2.0 g (2.49 mmol) of **3-12-*p***, 0.72 cm^3 (7.47 mmol) of methacryloyl chloride, and 1.04 cm^3 (7.47 mmol) of Et_3N, were obtained 1.31 g (60.4%) of a clear liquid **4-12-*p***. Purity: 99% (HPLC), δ($CDCl_3$) 0.88 (t, 9 H, CH_3), 1.26 [overlapped peaks, 62 H, (CH_2)], 1.78 (overlapped peaks, 6 H, CH_2CH_2OPh and COOCH_2CH_2), 1.94 (s, 3 H, $CH_3C{=}CH_2$), 4.02 (t, 6 H, CH_2CH_2OPh, *J* 6.4), 4.14 (t, 2 H, $CH_2OOCCCH_3$, *J* 6.7), 4.29 (t, 2 H, COOCH$_2$, *J* 6.7), 5.55 [s, 1 H, C(CH$_3$)=CH_2 *trans* to C=O], 6.10 [s, 1 H, C(CH$_3$)=CH_2 *cis* to C=O], 7.26 (s, 2 H, ArHCOO); ν_{max}/cm^{-1} 1715 (C=O).

2-[2-(2-*Methacryloylethoxy*)*ethoxy*]*ethyl* 3,4,5-*tris*(n-*octadecan*-1-*yloxy*)*benzoate* (**4-18-3**). From 3.00 g (2.8 mmol) of **3-18-3**, 1.08 cm^3 (11.2 mmol) of methacryloyl chloride and 2.19 cm^3 (15.7 mmol) of Et_3N in 50 cm^3 of dry $CHCl_3$ were obtained 1.62 g (51.3%) of a white solid **4-18-3**. Purity: 99% (HPLC), m.p. 59 °C (DSC at 20 °C min^{-1}); δ($CDCl_3$) 0.88 (t, 9 H, CH_3), 1.26 [overlapped peaks, 90 H, $(CH_2)_{15}$], 1.77 (overlapped peaks, 6 H, CH_2CH_2OPh), 1.94 (s, 3 H, $CH_3C{=}CH_2$), 3.69–3.75 (overlapped peaks, 6 H, $CH_2CH_2OCH_2CH_2OOCCCH_3$), 3.83 (t, 2 H, PyCOOCH$_2CH_2$, *J* 5.0), 4.01 (overlapped peaks, 6 H, CH_2CH_2OPh), 4.30 (t, 2 H, $CH_2OOCCCH_3$, *J* 4.8), 4.46 (t, 2 H, COOCH_2, *J* 5.1), 5.57 (s, 1 H, C(CH$_3$)=CH_2 *trans* to C=O], 6.13 [s, 1 H, C(CH$_3$)=CH_2 *cis* to C=O], 7.27 (s, 2 H, ArHCOO); ν_{max}/cm^{-1} 1715 (C=O).

Free-radical Polymerization of **4-7-3**, **4-12-*n***, **4-12-*p*** *and* **4-18-3**. All polymerizations were carried out using the procedure described below. In a dry Schlenk tube fitted with a rubber septum were placed 0.85 g (0.97 mmol) of **4-12-13**, 0.0048 g (0.03 mmol) of AIBN and 4.0 cm^3 of freshly distilled benzene. The solvent was degassed by performing five freeze–pump–thaw cycles. The mixture was then stirred at 60 °C for 20–24 h after which the polymerization was quenched by exposure of the reaction mixture to air and dilution with further solvent. The polymer was purified by passing its light petroleum solution through a short column of neutral alumina. The unchanged monomer remains in the column. Yield: 0.47 g (55%). The characterization of the polymers is summarized in Table 2.

Complexes of **3-7-3**, **3-12-3**, **3-18-3** *and* **5-12-3** *with* $LiCF_2SO_3$.—All complexes were made using the following general procedure. In a vial were placed 0.030 g of the compound an an appropriate volume (indicated below) of a solution of $LiCF_3SO_3$ in dry THF. THF was then added so that all volumes were equal. The resultant solutions were then evaporated at room temperature under weak vacuum (> 10 mmHg) for 24 h, after which the complexes were further dried at 5×10^{-2} mmHg for 48 h at room temperature with a solid CO_2–acetone cooled trap attached. An example is as follows. A THF solution (0.10 cm^3) containing 5.35×10^{-4} g (0.0343 mol dm^{-3}) of $LiCF_3SO_3$ was added to 0.030 g (0.0343 mmol) of **5-12-3** to yield 0.10 mol of $LiCF_3SO_3$ per mole of **5-12-3**. The results of DSC analysis of the complexes are presented in Table 2 with the exception of the complexes of **3-7-3** which did not display any first-order transitions.

Results and Discussion

Scheme 2 outlines the synthesis of the monoesters (**3-*m*-*n***) of 3,4,5-tris(*n*-alkan-1-yloxy)benzoic acid (**1-*m***) with the non-selective oligo(oxyethylene) endo-receptors (**2-*n***) containing one, two, three and four repeat units, and of the monoester of 3,4,5-tris(*n*-dodecan-1-yloxy)benzoic acid (**1-12**) with the non-receptor octane-1,8-diol (**2-*p***), as well as of their corresponding polymethacrylates (**5-*m*-*n*** and **5-12-p**). 3,4,5-Tris(*n*-heptan-1-yloxy)-(**1-7**), 3,4,5-tris(*n*-dodecan-1-yloxy)-(**1-12**), and 3,4,5-tris(*n*-octadecan-1-yloxy)-(**1-18**) benzoic acids were synthesized according to previously reported procedures.[7] The synthesis of monoesters **3-7-3**, **3-12-*n***, **3-12-*p*** and **3-18-3** was accomplished by esterification under mildly basic reaction conditions. The methacrylate monomers (**4-7-3**, **4-12-*n***, **4-12-*p*** and **4-18-3**) were prepared by esterification of the corresponding monoesters with methacryloyl chloride in dry CH_2Cl_2 using Et_3N as the base. The polymethacrylates **5-7-3**, **5-12-*n***, **5-12-*p*** and **5-18-3** were obtained by free-radical polymerization of the monomers initiated with AIBN in dry benzene under an Ar atmosphere at 60 °C. All polymers were purified as described in the Experimental section until both GPC and NMR analysis showed that they were free of unpolymerized monomer.

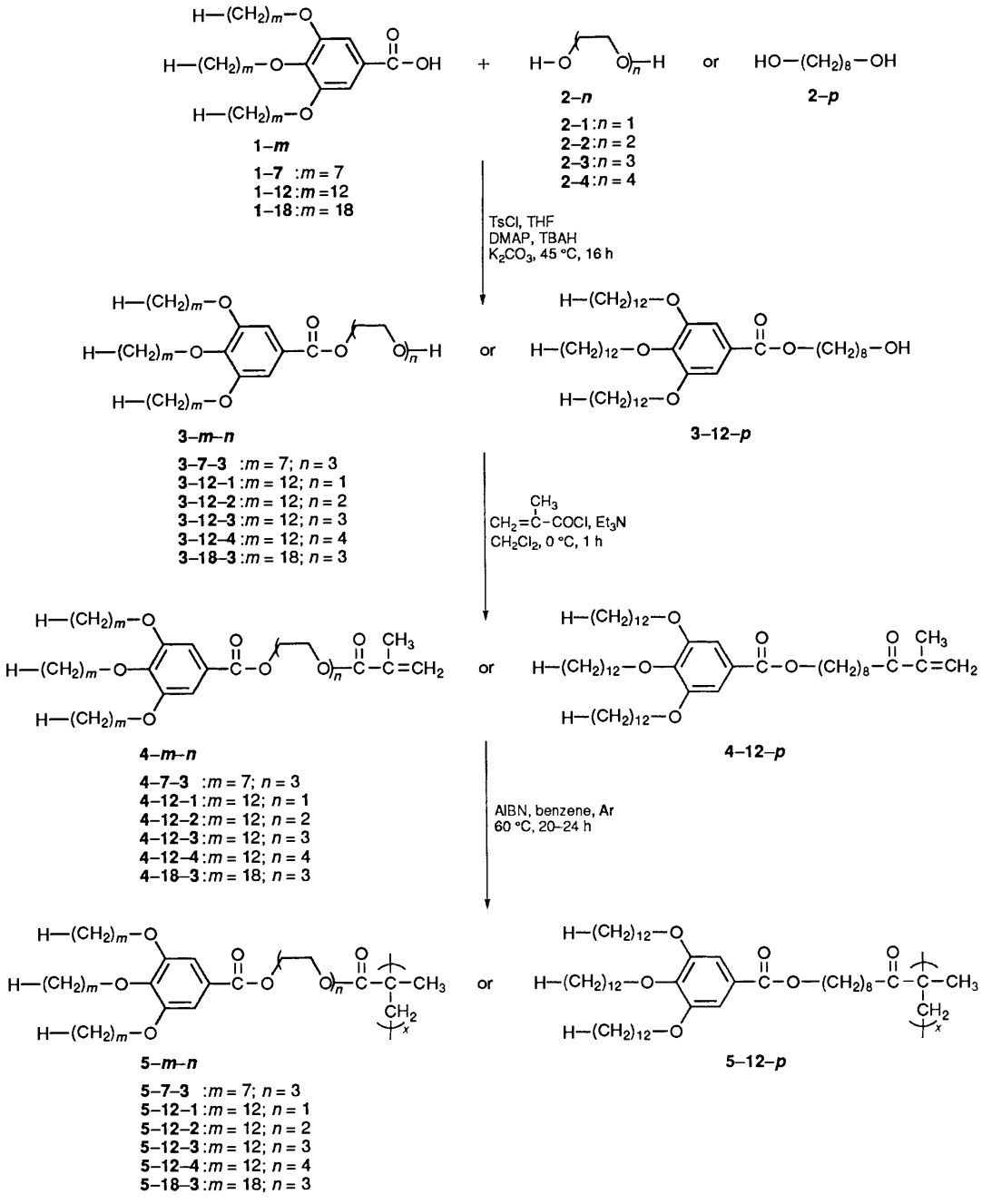

Scheme 2 Synthesis of ω-hydroxyoligo(oxyethylene) 3,4,5-tris(*n*-alkan-1-yloxy)benzoates (**3-7-3**, **3-12-*n***, **3-18-3**), of 1-hydroxy-8-octyl 3,4,5-tris-(*n*-dodecan-1-yloxy)benzoate (**3-12-*p***), and of their corresponding polymethacrylates (**5-7-3**, **5-12-*n***, **5-18-3**, **5-12-*p***)

The phase behaviour of low molar mass compounds, their polymethacrylates, and their complexes with $LiCF_3SO_3$ was characterized by a combination of techniques consisting of differential scanning calorimetry (DSC), thermal optical polarized microscopy and X-ray scattering experiments. The results of X-ray scattering characterization will be discussed in the second part of this paper.

The 3,4,5-tris(*n*-alkan-1-yloxy)benzoic acids **1-7**, **1-12** and **1-18** are crystalline only. Their corresponding monoesters with oligo(oxyethylene) endo-receptors are either crystalline (**3-12-1**, **3-12-2**, **3-12-3** and **3-18-3**) or amorphous (**3-7-3** and **3-12-*p***). This behaviour is in contrast with the behaviour of 3,4,5-tris[*p*-(*n*-dodecan-1-yloxy)benzyloxy]benzoic acid and its monoesters with oligo(oxyethylene) endo-receptors [Scheme 1(*a*), (*b*)].[3] The latter compounds self-assemble into a cylindrical supramolecular architecture that displays an enantiotropic columnar hexagonal (Φ_h) mesophase. This self-assembly is a result of a combination of endo-recognition provided by dipolar and hydrogen-bonding interactions of the oligo(oxyethylene) endo-receptor and exo-recognition provided by the pronounced taper shape of the DOBOB fragment.[3] The absence of a pronounced taper shape in the case of compounds based on the 3,4,5-tris(*n*-alkan-1-yloxy)benzoate fragment is most likely the reason for their markedly different phase behaviour.

Table 1 summarizes the phase transitions and associated enthalpy changes of the complexes of **3-12-3** and **3-18-3** as a function of the amount of $LiCF_3SO_3$. In both cases complexation of $LiCF_3SO_3$ by the oligo(oxyethylene) (OE) endo-receptor induces the formation of a hexagonal columnar (Φ_h) mesophase. The assignment of this mesophase was confirmed by X-ray scattering experiments. Fig. 1(*a*) and (*b*) plots the crystalline–Φ_h transition temperature (T_m) and Φ_h–isotropic transition temperature (T_i) of the complexes of **3-12-3** and **3-18-3** as a function of the $LiCF_3SO_3$ concentration. Uncomplexed

Table 1 Thermal transitions of the complexes of **3-12-3**, **3-18-3**, and **5-12-3** with various amounts of added $LiCF_3SO_3$ (Φ_h = hexagonal columnar mesophase; k_1, k_2 = crystalline phases; i = isotropic phase; c = crystallization occurs during heating). The data on the first line are from the first heating and the first cooling DSC scans and data on the second line are from the second heating DSC scans.

Compound	Moles of added $LiCF_3SO_3$	Thermal transitions (°C) and corresponding enthalpy changes (kcal mol)[a] in parentheses	
		Heating scan	Cooling scan
3-12-3	0.00	k 54 (28.0) i c 22 (−4.5) k_1 52 (26.0) i	i 10 (13.0) k_1
3-12-3	0.20	k 49 (26.6) i c 23 (−1.8) k_2 29 (2.7) c 32 (3.9) k_1 48 (22.7) i	i 18 (0.30) Φ_h 12 (14.3) k_1
3-12-3	0.40	k_1 47 (24.0) i k_2 27 (3.2) c 30 (−5.3) k_1 43 (15.7) i	i 34 (0.22) Φ^h 13 (12.7) k_1
3-12-3	0.60	k_1 36, 48 (25.4)[b] i k_2 29 (1.9) c 32 (−2.4) k_1 42 (12.2) i	i 46 (0.17) Φ_h 14 (12.6) k_1
3-12-3	0.80	k_1 46 (20.7) Φ_h 70 (0.09) i k_2 29 (1.5) c 33 (−1.9) k_1 40, 50 (11.8)[b] Φ_h 63 (0.10) i	i 57 (0.15) Φ_h 16 (12.6) k_1
3-12-3	1.00	k_1 46, 52 (18.9)[b] Φ_h 71 (0.07) i k_2 32 (3.3) c 34 (−2.0) k_1 39, 54 (10.8)[b] Φ_h 67 (0.12) i	i 62 (0.12) Φ_h 16 (10.8) k_1
3-12-3	1.20	k_1 50, 57 (19.6)[b] Φ_h 77 (0.09) i k_2 35 (2.7) c 36 (−4.3) k_1 42, 46 (15.1)[b] Φ_h 77 (0.12) i	i 71 (0.15) Φ_h 19 (12.1) k_1
3-18-3	0.00	k_1 75 (34.50) i k_2 62 (12.7) c 65 (−13.8) k_1 74 (26.8) i	i 52 (25.2) k_1
3-18-3	0.20	k_1 71 (18.4) i k_1 67 (16.5) i	8 50 (17.8) k_1
3-18-3	0.40	k_1 71 (20.7) i k_1 67 (17.5) i	i 58 (18.2) k_1
3-18-3	0.60	k_1 75 (21.8) i k_1 71 (17.8) i	i 61 (16.9) k_1
3-18-3	0.80	i_1 75 (26.7) i k_1 72 (16.5) i	i 62 (14.9) k_1
3-18-3	1.00	k_1 73, 82 (28.7)[b] Φ_h 97 (0.04) i k_2 66, 74 (14.8)[b] k_1 80 (0.53) Φ_h 94 (0.08) i	i 86 (0.12) Φ_h 63 (13.5)[b] k_1
3-18-3	1.20	k_1 65, 73, 83 (26.9)[b] Φ_h 108 (0.24) i k_2 66, 75 (14.0)[b] k 81 (0.69) Φ_h 105 (0.10) i	i 97 (0.13) Φ_h 64 (13.1)[b] k_1
3-18-3	1.40	k_2 72, 86, 99 (26.4)[b] Φ_h 126[c] i k_2 65, 77, 82 (14.6)[b] Φ_h 122 (0.03) i	i 118 (0.05) Φ_h 63 (13.1)[b] k_1
3-18-3	1.60	k_2 65, 72, 85 (25.3)[b] k 96 (2.34) Φ_h 132[c] i k_2 64, 77 (13.5)[b] k 81.92 (1.38) Φ_h 127 (0.04) i	i 128[c] Φ_h 64 (12.7)[b] k_1
3-18-3	1.80	k_2 65, 71, 85 (23.8)[b] k_1 97 (1.81) Φ_h 126 (0.04) i k_2 66, 77, 82 (12.7)[b] k_1 96 (0.47) Φ_h 122 (0.03) i	i 120 (0.12) Φ_h 62 (12.5) k_1
3-18-3	2.00	k_2 56, 66, 72, 83 (26.1)[b] k_1 94 (2.18) Φ_h 128[c] i k_1 66, 77, 82 (14.5)[b] k_1 97 (0.74) Φ_h 128 (0.05) i	i 121 (0.09) Φ_h 63 (13.8) k_1
5-12-3	0	k_1 16 (5.7) Φ_h 52 (0.09) i k_1 15 (5.1) Φ_h 51 (0.09) i	i 31 (0.09) Φ_h 2 (4.9) k_1
5-12-3	0.1	k_1 16 (4.4) Φ_h 60 (0.18) i k_1 16 (4.6) Φ_h 58 (0.18) i	i 38 (0.13) Φ_h 3 (4.4) k_1
5-12-3	0.2	k_1 16 (4.0) Φ_h 64 (0.16) i k_1 16 (4.2) Φ_h 62 (0.15) i	i 41 (0.14) Φ_h 2 (4.0) k_1
5-12-3	0.3	k_1 15 (3.5) Φ_h 65 (0.12) i k_1 16 (4.1) Φ_h 63 (0.09) i	i 41 (0.13) Φ_h 2 (3.6) k_1
5-12-3	0.4	k_1 16 (3.6) Φ_h 65 (0.14) i k_1 16 (3.9) Φ_h 62 (0.14) i	i 42 (0.12) Φ_h 2 (3.5) k_1
5-12-3	0.5	k_1 15 (3.6) Φ_h 64 (0.13) i k_1 15 (3.8) Φ_h 62 (0.12) i	i 42 (0.12) Φ_h 2 (3.5) k_1
5-12-3	0.6	k_1 15 (3.5) Φ_h 65 (0.19) i k_1 16 (3.8) Φ_h 63 (0.11) i	i 43 (0.11) Φ_h 3 (3.4) k_1
5-12-3	0.7	k_1 16 (3.5) Φ_h 63 (0.11) i k_1 16 (3.9) Φ_h 62 (0.14) i	i 43 (0.13) Φ_h 3 (3.4) k_1
5-12-3	0.8	k_1 16 (3.5) Φ_h 63 (0.19) i k_1 17 (3.8) Φ_h 62 (0.11) i	i 42 (0.11) Φ_h 3 (3.1) k_1
5-12-3	0.9	k_1 16 (3.7) Φ_h 64 (0.17) i k_1 16 (3.5) Φ_h 59 (0.10) i	i 39 (0.10) Φ_h 2 (3.3) k_1
5-12-3	1.0	k_1 16 (3.9) Φ_h 63 (0.20) i k_1 16 (3.8) Φ_h 59 (0.14) i	i 40 (0.12) Φ_h 3 (3.3) k_1

[a] The molecular weight is weight averaged with the amount of $LiCF_3SO_3$ present. [b] Combined enthalpies for overlapped transitions are presented. [c] The transition was undectable by DSC and the temperature was assigned by thermal optical polarized microscopy at 20 °C min^{-1}.

3-12-3 is only crystalline. The addition of 0.2 mol of $LiCF_3SO_3$ results in the formation of a monotropic Φ_h mesophase. T_i of the $LiCF_3SO_3$ complexes of **3-12-3** systematically increases with the increase in the amount of $LiCF_3SO_3$. At concentrations above 0.8 mol of $LiCF_3SO_3$ per mole of **3-12-3** the Φ_h mesophase becomes enantiotropic [Figs. 1(*a*) and (*b*)]. The complex appears to become biphasic above a concentration of 1.2 mol of $LiCF_3SO_3$. Thermal optical polarized microscopy shows that both isotropic and anisotropic phases seem to be present.

Similar behaviour is exhibited by compound **3-18-3** and its $LiCF_3SO_3$ complexes. However, in this case the formation of

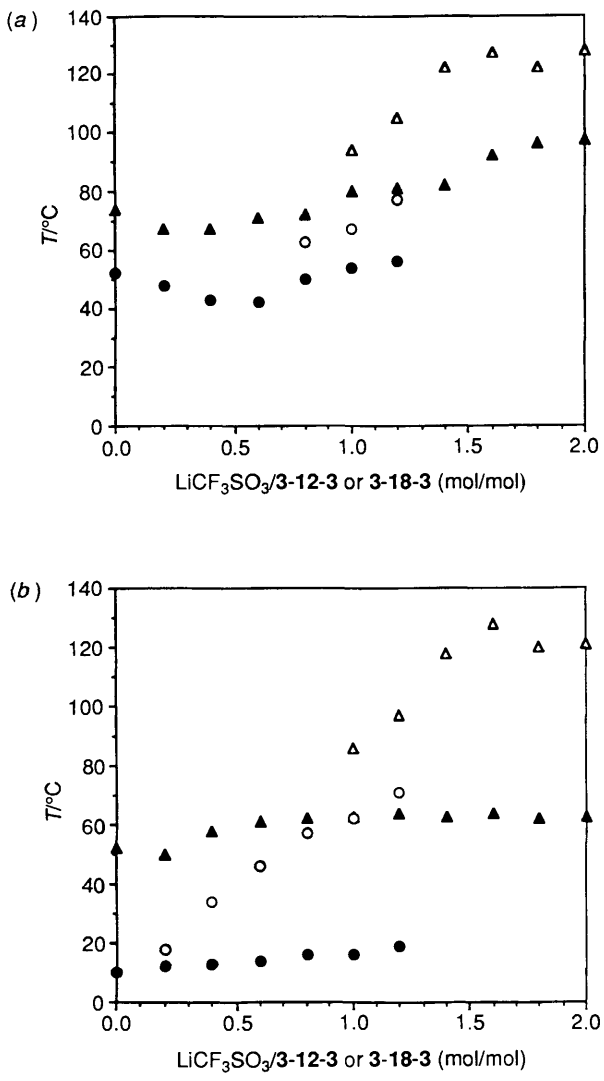

Fig. 1 The dependence of: T_m (filled symbols) and T_i (open symbols) phase transition temperatures of the complexes of **3-12-3** (○, ●) and **3-18-3** (△, ▲) as a function of the amount of $LiCF_3SO_3$ in the complex obtained from (*a*) second DSC heating scan; (*b*) first DSC cooling scan

the Φ_h mesophase requires at least 1.0 mol of $LiCF_3SO_3$. This can be attributed to the higher crystal stability of the octadecyl aliphatic tails. The T_i of the complexes of **3-18-3** reaches a maximum at about 1.5 mol of $LiCF_3SO_3$ and thereafter remains relatively constant up to the onset of phase separation (*ca.* 2.0 mol $LiCF_3SO_3$). For the same $LiCF_3SO_3$ concentration (*e.g.*, 1.2 mol of $LiCF_3SO_3$) in their complexes, **3-18-3** has a T_i (105 °C) which is higher by 28 °C than the T_i (77 °C) of **3-12-3** [Fig. 1(*a*)]. For the same increase in $LiCF_3SO_3$ concentration (from 1.0 to 1.2 mol of $LiCF_3SO_3$) both **3-12-3** and **3-18-3** complexes show the same relative increase in T_i (about 10 °C). The T_m of the complexes of **3-12-3** and **3-18-3** with $LiCF_3SO_3$ is not affected very much by the amount of $LiCF_3SO_3$. In contrast with the behaviour of the complexes of **3-12-3** and **3-18-3**, the $LiCF_3SO_3$ complexes of **6** are only isotropic up to high salt concentrations (*ca.* 1.5–2.0 mol of $LiCF_3SO_3$) where a salt-induced crystalline phase is indicated by DSC analysis. Similar behaviour is presented in detail elsewhere.[8]

It is important to mention that the addition of $LiCF_3SO_3$ for these compounds, does not result in any detectable decomposition. Previous $LiCF_3SO_3$ complexation experiments of the monoesters of 3,4,5-tris[*p*-(dodecan-1-yloxy)benzyloxy]benzoic acid with OE endo-receptors have led us to suggest the possibility of Lewis acid (*i.e.*, $LiCF_3SO_3$) induced decomposition of their benzyl ether moieties.[3,8] The absence of any detectable $LiCF_3SO_3$-induced decomposition in the present system which lacks the benzyl ether moiety further supports our original assumption.[3,8]

The phase behaviour of all polymers is summarized in Table 2. Only the polymethacrylates **5-12-*n*** with n = 1, 2, 3 and 4 display a Φ_h mesophase. Polymers **5-7-3** and **5-12-*p*** are amorphous (Table 2, Fig. 2). In contrast with **5-12-*n***, polymer **5-18-3** is only crystalline (Table 2). Most probably, this polymer exhibits a virtual Φ_h mesophase that is covered by the crystalline phase. A detailed discussion of virtual mesophases in liquid crystalline polymers and their thermodynamic interpretation is presented elsewhere.[9]

Fig. 2 presents the DSC traces of the polymethacrylates **5-12-*n*** determined from the first heating [Fig. 2(*a*)], the first cooling [Fig. 2(*b*)] and the second heating scans [Fig. 2(*c*)]. Polymers **5-12-1** and **5-12-2** display the Φ_h mesophase only in their first heating scans [Fig. 2(*a*)]. Subsequent heating and cooling scans display only the melting and crystallization transitions [Figs. 2(*b*) and (*c*)]. An attempt to recover the Φ_h mesophase of **5-12-1** by annealing the sample at room temperature for several hours was unsuccessful. The Φ_h phase of **5-12-2** was recovered after annealing for a short period of time (*ca.* 2 h). Polymers **5-12-3** and **5-12-4** display an enantiotropic Φ_h mesophase irrespective of their thermal history. **5-12-3** and **5-12-4** exhibit a stabilized Φ_h phase most probably due to the greater number of dipolar interactions generated by their OE segments and to the increase in polarity of the inner core. The one OE repeat spacer in **5-12-1** separates the taper side group from the rigid polymethacrylate backbone by only two atoms. Most likely, the polymer backbone exerts a kinetic effect constraint on the formation of the Φ_h phase since the taper side groups have to accommodate both its steric and conformational requirements. The validity of this statement is supported by the experimentally observed enhanced ease of formation of the Φ_h phase on going from one to four OE repeat units in the spacer.

The DSC traces of the amorphous polymer **5-12-*p*** are compared with those of polymer **5-12-3** in Fig. 2. The OE endo-receptor in **5-12-3** is replaced by an eight-methylene spacer resulting in polymer **5-12-*p***. The replacement of the polar OE endo-receptor by the non-polar aliphatic spacer results in complete suppression of both T_i and T_m. Therefore, the presence of the flexible OE spacer is essential for the formation of both Φ_h and crystalline phases.

T_m and T_i of polymethacrylates **5-12-*n*** are plotted in Fig. 3 as a function of the number of OE repeats in the flexible spacer. The plotted data were determined from first heating DSC scans since **5-12-1** and **5-12-2** display the T_i transition only during these scans. T_m increases with the increase in the number of repeat units in the OE spacer. However, to within experimental error, T_i is relatively constant and independent of the length of the OE spacer.

Figs. 4(*a*) and (*b*) compare the T_m and T_i of the complexes of **3-12-3** with those of the corresponding polymer **5-12-3** as a function of $LiCF_3SO_3$ concentration. Both **3-12-3** and **5-12-3** have three OE repeat units in the spacer. The thermal transitions of the complexes of the polymer **5-12-3** are summarized in Table 1. While **3-12-3** can complex up to 1.2 mol of $LiCF_3SO_3$, **5-12-3** can complex a maximum of 0.3 mol of $LiCF_3SO_3$. Above this concentration, T_i reaches a plateau with the concurrent presence of anisotropic aggregates that persist above T_i. As observed by optical microscopy these aggregates appear to be a mixture of crystalline and Φ_h phases. The T_m of the complexes of **5-12-3** is essentially independent of the amount of $LiCF_3SO_3$ [Figs. 4(*a*) and (*b*)]. The data collected from the cooling DSC scans [Fig. 4(*b*)] enable us to make a comparison between the 'molecular' (covalent) backbone of

Table 2 Characterization of polymethacrylates **5-7-3**, **5-12-*n***, **5-12-*p*** and **5-18-3** (Φ_h = hexagonal columnar mesophase; k_1 = crystalline phase; i = isotropic phase). Data on the first line are from the first heating and cooling scans and data on the second line are from the second heating scans.

Polymer	GPC $M_n \times 10^{-3}$	GPC M_w/M_n	Yield (%)	Thermal transitions (°C) and corresponding enthalpy changes (kcal mol^{-1}) in parentheses: Heating	Cooling
5-7-3	153.7	1.30	70	i i	
5-12-1	57.2	1.64	54	k_1 −9 (1.50) Φ_h 51 (0.16) i k_1 −10 (1.28) i	i > −20 k_1
5-12-2	69.9	1.75	78	k_1 6 (3.48) Φ_h 51 (0.18) i k_1 6 (3.28) i	i −5 (2.67) k_1
5-12-3	43.1	1.90	55	k_1 16 (5.70) Φ_h 52 (0.09) i k_1 15 (5.14) Φ_h 51 (0.09) i	i 31 (0.09) Φ_h 2 (4.86) k_1
5-12-4	46.0	2.67	47	k_1 17 (6.05) Φ_h 54 (0.20) i k_1 17 (6.53) Φ_h 54 (0.16) i	i 37 (0.23) Φ_h 3 (5.88) k_1
5-12-*p*	38.3	1.37	62	i i	i
5-18-3	31.6	1.63	31	k_1 57 (15.34) i k_1 57 (15.41) i	i 43 (14.93) k_1

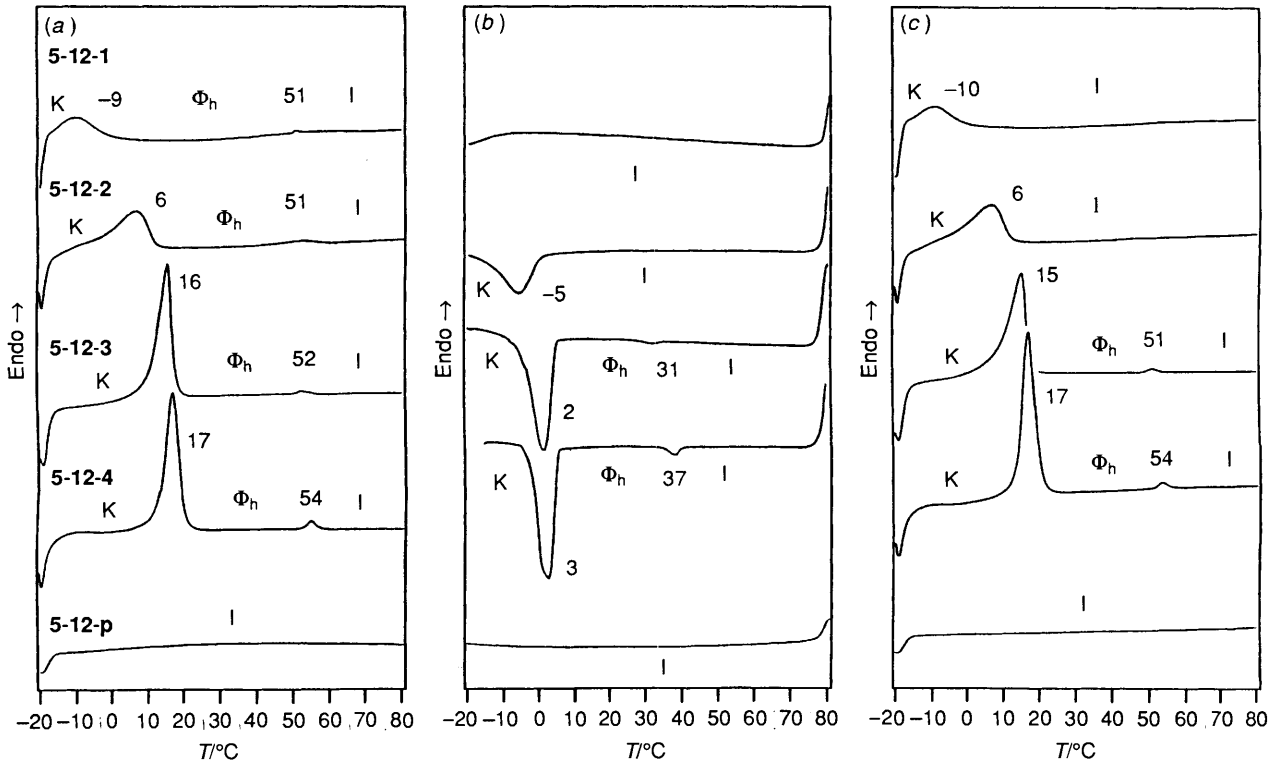

Fig. 2 DSC traces (20 °C min^{-1}) of **5-12-1**, **5-12-2**, **5-12-3**, **5-12-4** and **5-12-*p*** recorded during (*a*) first heating; (*b*) first cooling; (*c*) second heating scans

5-12-3 and the 'supramolecular backbone' which results from coordinate (non-covalent) bonding interactions of the OE receptor of **3-12-3** with Li^+ ions. T_i for the uncomplexed polymer **5-12-3** is 31 °C [Fig. 4(*b*)]. A T_i of the same value for the complex of **3-12-3** with $LiCF_3SO_3$ requires about 0.35 mol of $LiCF_3SO_3$ per mole of **3-12-3** [Fig. 4(*b*)]. Therefore, the complexation of 0.35 mol of $LiCF_3SO_3$ by **3-12-3** substitutes for the polymer backbone in **5-12-3**.

Representative textures of the Φ_h phases exhibited by the complex of **3-12-3** with 1.0 mol of $LiCF_3SO_3$, the complex of **3-18-3** with 1.0 mol of $LiCF_3SO_3$, the polymer **5-12-3**, and its complex with 0.2 mol of $LiCF_3SO_3$ are presented in Fig. 5. The textures of the complexes of **3-12-3** and **3-18-3** form faster and with considerably larger domains than those of the polymer **5-12-3** and its complex.

The complex of **3-12-3** with 1.0 mol of $LiCF_3SO_3$ and the polymers **5-12-1**, **5-12-2**, **5-12-3** and **5-12-4** were characterized by small-angle and wide-angle X-ray scattering experiments at various temperatures within their Φ_h mesophase. The *d*-spacings of all reflections are summarized in Table 3. The presence of strong sharp reflections at ratios of $d_0:d_1:d_2 = 1:1/\sqrt{3}:1/2$ with only a diffuse scattering at wide angles supports the assignment of a Φ_h mesophase.[1,2,10,11] Table 3 also lists the radii (R) of the cylindrical columns as calculated from the X-ray reflections ($R = a/2$, where a is the hexagonal unit cell parameter). Fig. 6 plots the experimentally determined column diameters ($2R = a$) of the complex of **3-12-3** with 1.0 mol of $LiCF_3SO_3$ and of the polymers **5-12-*n*** as a function of the number of OE repeats ***n*** in the endo-receptor. The column radius systematically increases with the increase in the number

(*a*)

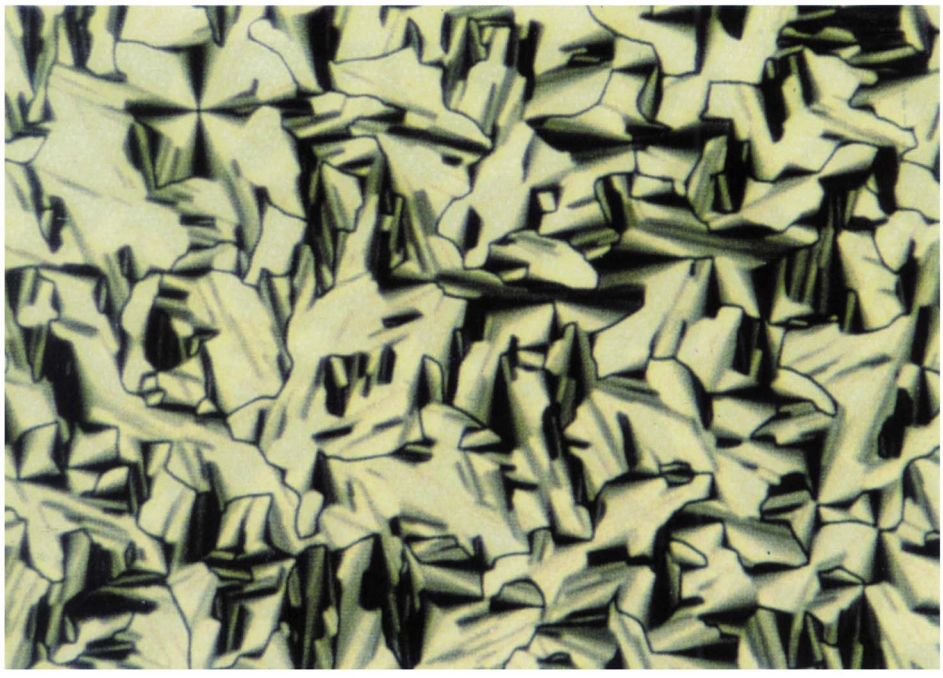

(*b*)

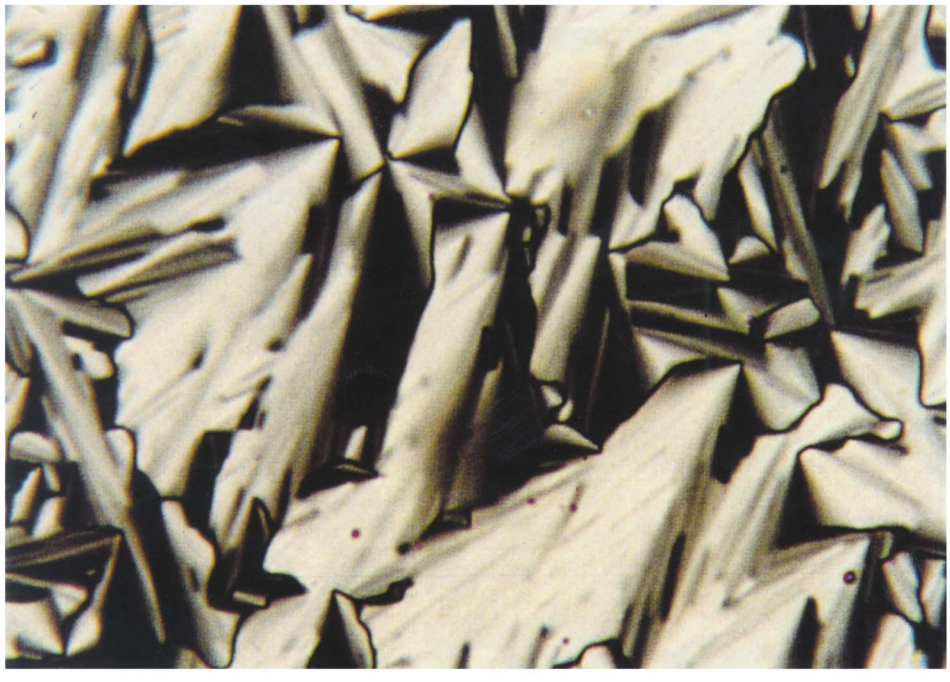

Fig. 5 Representative optical polarized micrographs of the texture exhibited by the hexagonal columnar (Φ_h) mesophase of (*a*) the complex of **3-12-3** with 1.0 mol of $LiCF_3SO_3$ upon cooling from 80 °C to 70 °C (1 °C min^{-1}); (*b*) the complex of **3-18-3** with 1.0 mol of $LiCF_3SO_3$ upon cooling from 95 °C to 87 °C (1 °C min); (*c*) **5-12-3** upon cooling from 55 °C to 27 °C (0.1 °C min^{-1}); (*d*) the complex of **5-12-3** with 0.2 mol of $LiCF_3SO_3$ upon cooling from 70 °C to 35 °C (0.1 °C min^{-1})

[To face p. 38]

(*c*)

(*d*)

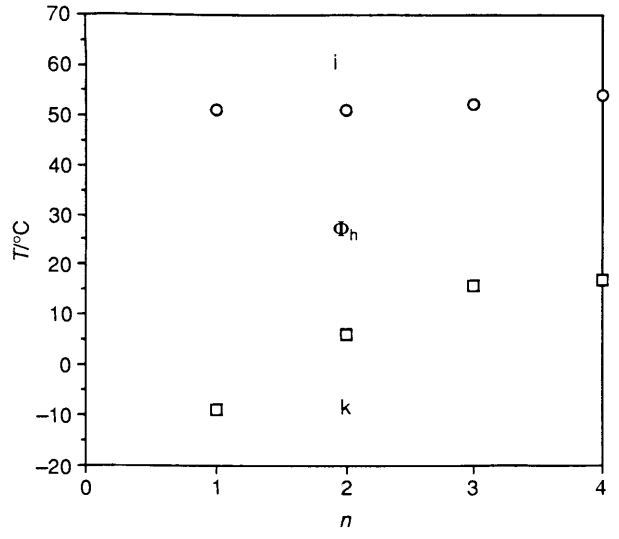

Fig. 3 The dependence of the T_m (□) and T_i (○) phase-transition temperatures of polymers **5-12-3** *versus* the number of OE repeat units (***n***) in the flexible spacer (data from the first heating DSC scan, Table 2)

of OE repeat units. The complex of **3-12-3** with 1.0 mol of $LiCF_3SO_3$ has a radius that is 1.2 Å smaller than that of its corresponding uncomplexed polymer **5-12-3**. Fig. 6 also plots the column diameters of the polymethacrylates based on 3,4,5-tris[*p*-(*n*-dodecan-1-yloxy)benzyloxy]benzoate (DOBOB) groups with an OE spacer as a function of the number of OE repeat units in its endo receptor.[3] These compounds also self-assemble into cylindrically shaped architectures. The diameters of the polymers based on the DOBOB tapered groups have larger column diameters than the columns of the analogous polymers **5-12-*n***. This increase is consistent with the expected change that should occur with the benzyl ether groups present in the DOBOB tapers.

Using the experimentally determined densities (ρ) of polymers **5-12-*n***, which are also summarized in Table 3, and the calculated value of the distance from the column centre to the hexagon vertex S ($S = 2R/\sqrt{3}$), we can calculate the number of polymer repeat units (μ) of **5-12-*n*** that are present in a cross-section layer of 3.74 Å thickness of the column [2,12] by using eqn. (1), where μ is the number of repeat units of **5-12-*n*** in a cross-

$$\rho = \frac{2\mu M}{3\sqrt{3}N_A S^2 t} \quad (1)$$

section, M is the molecular weight of the polymer repeat unit, N_A is Avogadro's number ($6.022\,045 \times 10^{23}$) and $t = 3.74 \times 10^{-8}$ cm. A more detailed discussion of this calculation has been presented previously.[2] The results of this calculation are also summarized in Table 3. **5-12-1** has about four repeat units per cross-section, while **5-12-2**, **5-12-3** and **5-12-4** have about five repeat units per cross-section.

Molecular modelling was used to construct models of the cross-section of the thermotropic cylindrical inverse micelle-like supramolecular architecture would would result from the self-assembly of the $LiCF_3SO_3$ complexes of **3-7-3** [Fig. 7(*a*)], **3-12-3** [Fig. 7(*b*)], and **3-18-3** [Fig. 7(*c*)]. All models were constructed having five taper-shaped molecules per cross-section based on the above calculations for the polymers. The inner core of the column is constituted by the OE segments as a result of dipolar interactions and microsegregation from the hydrophobic aliphatic tails. The inner core is further stabilized by the presence of Li^+ cations (represented as filled atoms) within Van der Waals radii of at least two donor oxygen atoms (represented as spotted atoms) of the OE spacers. The OE spacers were

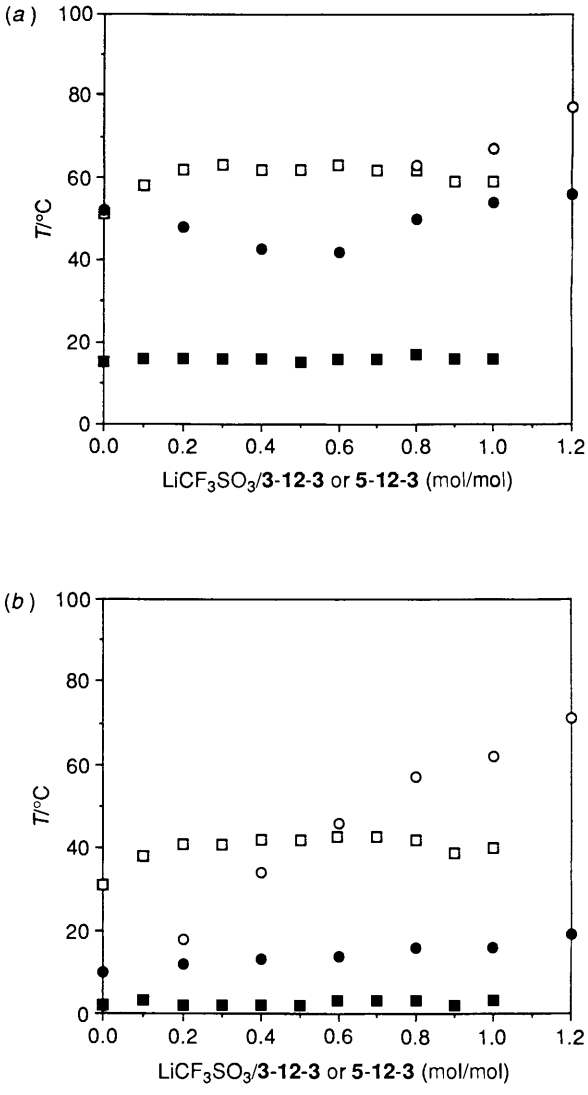

Fig. 4 The dependence of T_m (filled symbols) and T_i (open symbols) phase-transition temperatures of the complexes of **3-12-3** (○, ●) and **5-12-3** (□, ■) as a function of the amount of $LiCF_3SO_3$ in the complex obtained from (*a*) a second DSC heating scan; (*b*) first DSC cooling scan

arbitrarily melted in a two-dimensional (2-D) cross-section using standard bond lengths and angles so that the space in the inner core was efficiently filled. This provides an arrangement in which the most probable coordination site for four of the six Li cations is between an OE oxygen atom and a carbonyl oxygen atom. Previously, random melting of the OE spacer provided that all complexation sites within a 2-D cross-section were only between donor oxygen atoms of the OE spacer.[8] Increased rigidity of the inner core arises from the decrease in the conformational mobility of the OE receptor by complexation, and from the increase in its polarity. The increase of the polarity of the inner core is a result of its transformation from a dipolar medium into an ionic medium which enhances its microsegregation from the outer non-polar aliphatic core. The number of Li^+ cations present in the inner core of the model is in agreement with the experimentally determined value of 1.2 mol of $LiCF_3SO_3$ per mole of **3-12-3**. Exo-recognition is most likely provided by the hydrophobic effect and the conformational disorder of the melted aliphatic tails which radiate towards the periphery of the column. The combination of endo-recognition (provided by the ionic interactions) and exo-recognition (provided by the taper shape) constitutes the driving force for

the cylindrical inverse micelle-like self-assembly. The formation of lyotropic hexagonal columnar liquid crystalline phases by cylindrical inverse micelle assemblies is well-documented.[13]

Fig. 7(*a*) illustrates a model of the cross-section of five molecules of the $LiCF_3SO_3$ complex of **3-7-3** in the same self-assembled shape. While endo-recognition is present, the short aliphatic tails most likely cannot assume an efficient taper shape or do not have the necessary hydrophobic character to provide exo-recognition for the stabilization of this cylindrical assembly.

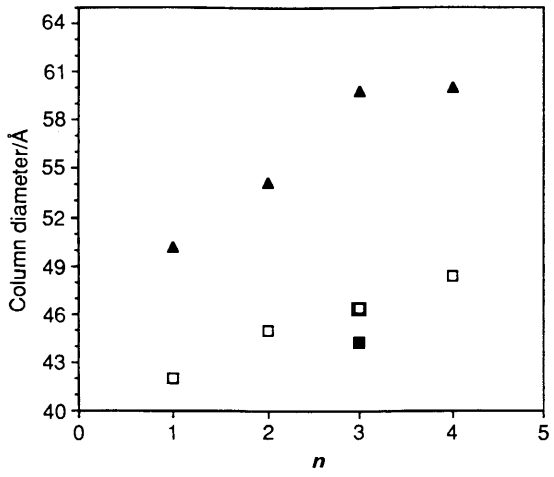

Fig. 6 The dependence of the column radius of **3-12-3** with 0.3 mol of $LiCF_2SO_3$ (■), of **5-12-*n*** (□), and of DOBOB polymers (▲) in the Φ_h phase *versus* the number of OE repeat units (***n***) (data from Table 3 and ref. 3)

In contrast, both compounds **3-12-3** and **3-18-3** have longer aliphatic tails that can most likely assume a taper shape *via* their conformational disorder and also possess a greater hydrophobic character which enhances the microsegregation. Both complexes of **3-12-3** and **3-18-3** with $LiCF_3SO_3$ can self-assemble into the cylindrical arrangement [Figs. 7(*b*) and (*c*), respectively]. The aliphatic tails of the $LiCF_3SO_3$ complex of **3-12-3** are randomly melted in order for the cross-section diameter to agree with the experimentally determined value of 44.3 Å from the X-ray scattering experiments [Fig. 7(*b*), Table 3)]. Since the complex of **3-18-3** has a higher aliphatic content than the complex of **3-12-3**, the stability of its Φ_h mesophase at the same $LiCF_3SO_3$ concentration is greater (Fig. 1, Table 1).

Similar representative molecular models of the cross-section of the cylindrical assembly of polymers **5-12-1** and **5-12-3** are shown in Figs. 8(*a*) and (*b*). The models of **5-12-1** and **5-12-3** were constructed with four and five repeat units in their cross-sections in accordance with the experimental results obtained from X-ray scattering and density measurements. Their aliphatic tails were randomly melted so that their diameters match the experimentally measured values. The inner cores of the assembly of **5-12-1** and **5-12-3** consist of the polymethacrylate backbone and the OE segment of one and three repeat units, respectively [Figs. 8(*a*) and (*b*)]. The positional restrictions imposed on the OE spacer of **5-12-1** by its covalent attachment to the polymer backbone and to the bulky taper side group decreases its conformational mobility. It is not surprising that the Φ_h phase of **5-12-1** does not reform once the polymer is heated above its isotropization temperature (Table 2,

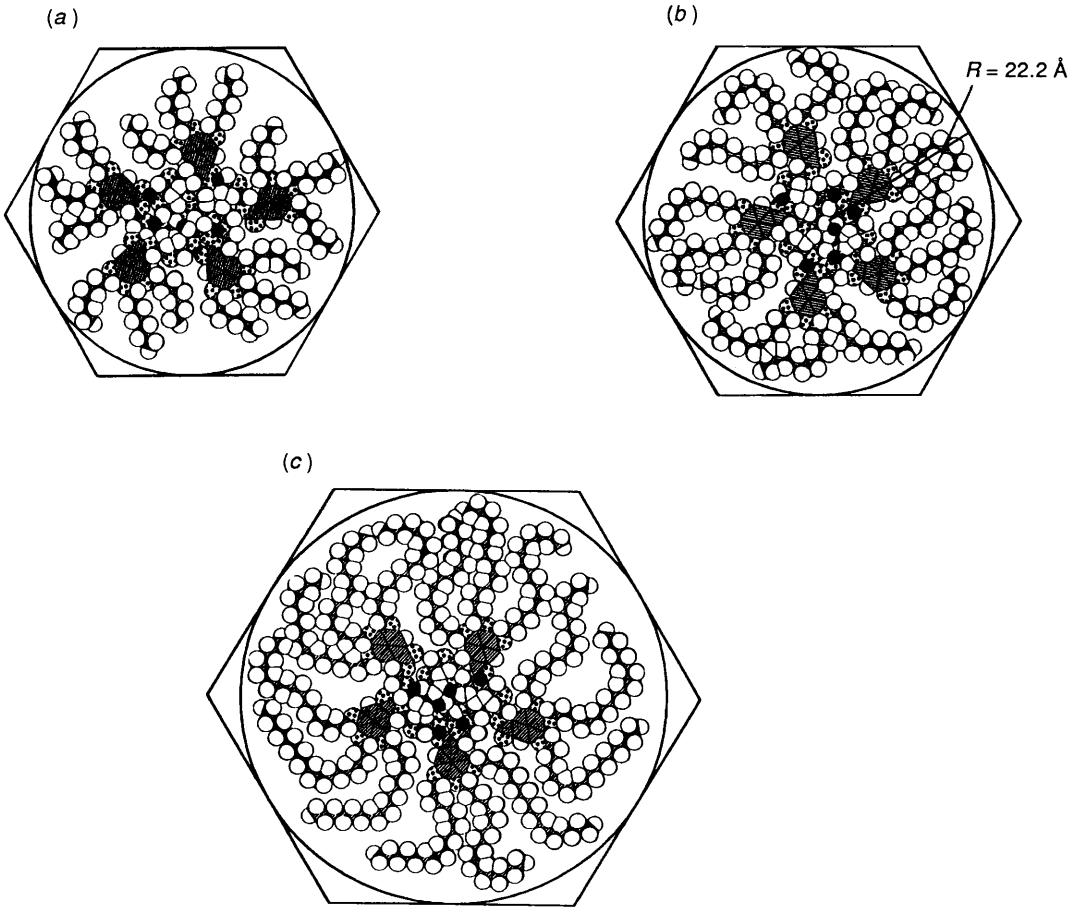

Fig. 7 Schematic representation of the supramolecular cylinders of monoesters of **1-7**, **1-12**, and **1-18** with OE receptors in the Φ_h mesophase: (*a*) top view of the cylinder containing five molecules of **3-7-3** in a cross-section layer; (*b*) top view of the cylinder containing five molecules of **3-12-3** in a cross-section layer with the alkyl tails melted to match the average column radius determined by X-ray scattering experiments; (*c*) top view of the cylinder containing five molecules of **3-18-3** in a cross-section layer

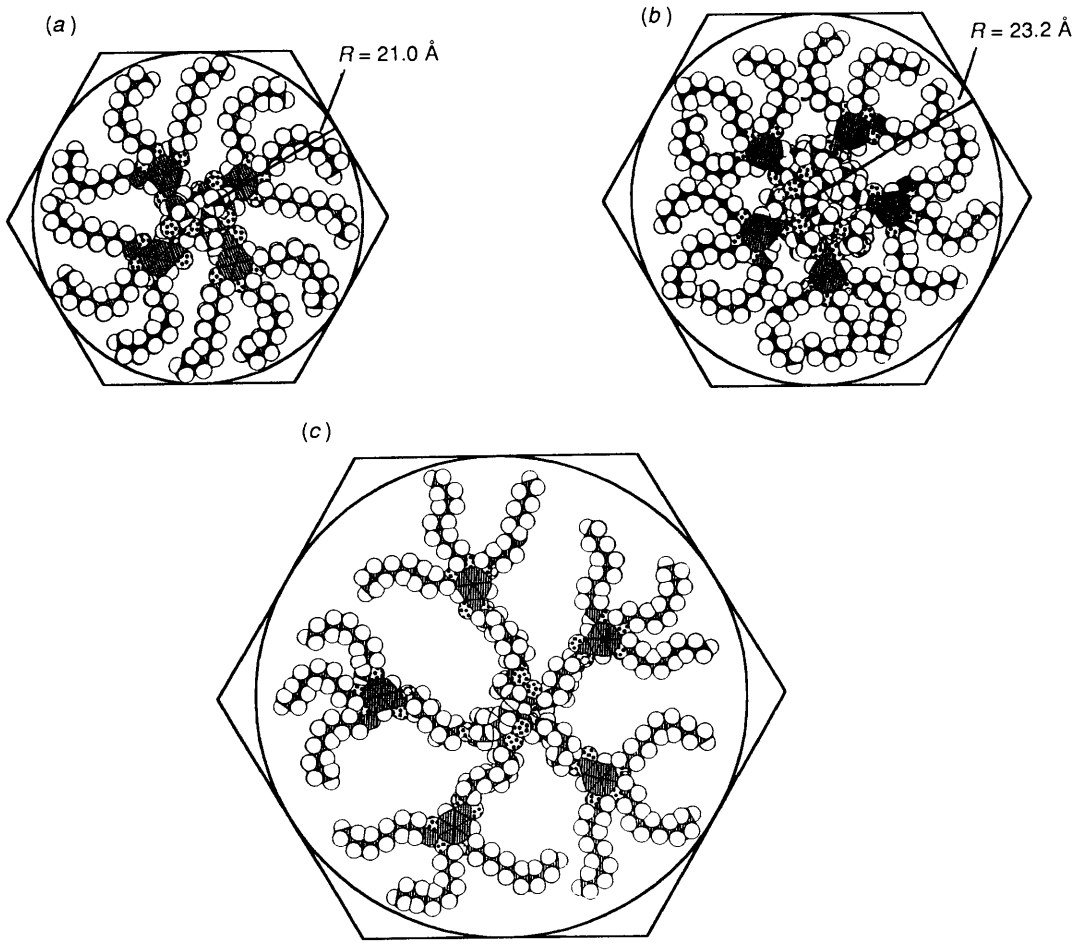

Fig. 8 Schematic representation of the supramolecular cylinders of the polymethacrylates based on **1-12** with OE receptors in the Φ_h mesophase: (*a*) top view of the cylinder containing four repeat units of **5-12-1** in a cross-section layer with the alkyl tails melted to match the average column radius determined by X-ray scattering experiments; (*b*) top view of the cylinder containing five repeat units of **5-12-3** in a cross-section layer with the alkyl tails melted to match the average column radius determined by X-ray scattering experiments; (*c*) top view of the cylinder containing five repeat units of **5-12-*p*** in a cross-section layer

Table 3 Characterization of the Φ_h phase of compounds **3-12-3** and **5-12-*n*** by X-ray scattering experiments

								Lattice parameter			
Compound	T/°C	d_{100}/Å	d_{110}/Å	d_{200}/Å	d_{210}/Å	$\langle d_{100}\rangle$/Å[a]	a/Å[b]	R/Å[b]	S/Å[b]	ρ[c]/g cm^{-3}[c]	μ[d]
3-12-3 + 1.0 mol of $LiCF_3SO_3$	64	—[e]	22.0	19.3	—[f]	38.4	44.3	22.2	25.6	—	—
5-12-1	27	36.4	—[f]	—[f]	—[f]	36.4	42.0	21.0	24.2	0.95	4.1
5-12-2	30	40.0	22.1	19.7	—[f]	39.0	45.0	22.5	26.0	0.97	4.6
5-12-3	27	40.0	23.2	20.3	—[f]	40.2	46.4	23.2	26.8	0.90	4.3
5-12-4	27	42.1	24.2	21.1	15.7	41.9	48.4	24.2	27.9	0.99	4.9
5-12-4	41	40.8	23.6	20.6	15.4	40.9	47.2	23.6	27.3	—	—

[a] $\langle d_{100}\rangle = (d_{100} + d_{110} \times \sqrt{3} + d_{200} \times 2)/3$. [b] $a = 2\langle d_{100}\rangle/\sqrt{3}$, $R = \langle d_{100}\rangle/\sqrt{3}$, $S = 2 \times R/\sqrt{3}$. [c] ρ = Experimental density at 20 °C. [d] μ = Number of monomer units per column stratum. [e] The reflection is strong but not sharp. [f] The reflection is absent.

Fig. 3). The OE segment of **5-12-3** is also covalently bonded to a polymethacrylate backbone and therefore, similar positional restrictions are imposed, but the longer length of the OE spacer has fewer conformational restrictions.

Furthermore a longer spacer can assume the required conformations for maximizing the dipolar interactions between OE segments. This may stabilize the cylindrical assembly of **5-12-3**. However, the experimental fact is that T_i does not change with the number of OE segments (***n***) in the spacer (Fig. 3, Table 2). One possible way of reconciling this apparent contradiction, *i.e.*, an increasing degree of dipolar interactions with a constant T_i, is by assuming a larger isotropization entropy for polymers with larger ***n***. The latter would not be an unreasonable assumption considering the higher overall flexibility of polymers with longer flexible spacers. Accordingly, the effects of higher dipolar interaction in the Φ_h phase (hence higher ΔH_i) and that of higher ΔS_i for polymers with larger ***n***, would cancel out and, due to $T_i = \Delta H_i/\Delta S_i$, leave T_i unchanged.

The positional restrictions imposed by the polymer backbone also influence the ability of the inner core of **5-12-3** to accommodate a large amount of salt. Consequently, it presents a greatly reduced $LiCF_3SO_3$ complexation ability when compared with its low molecular weight hydroxy terminated analogue **3-12-3** (Fig. 4).

Fig. 8(*c*) shows a model of the cross-section of the cylinder that would arise from the inverse micellar-like assembly of **5-12-*p***. As determined experimentally, **5-12-*p*** cannot form a Φ_h mesophase. The replacement of the OE endo-receptor by an aliphatic spacer of the same number of atoms removes the endo-recognition ability that results from the dipolar interactions of OE spacers. Exo-recognition provided by the conformational disorder and hydrophobic interactions of the aliphatic tails is probably not adequate by itself to generate the cylindrical assembly of **5-12-*p*** (Table 2).

Fig. 9 shows a schematic representation of the self-assembled supramolecular architecture resulting from the alkali-metal ion

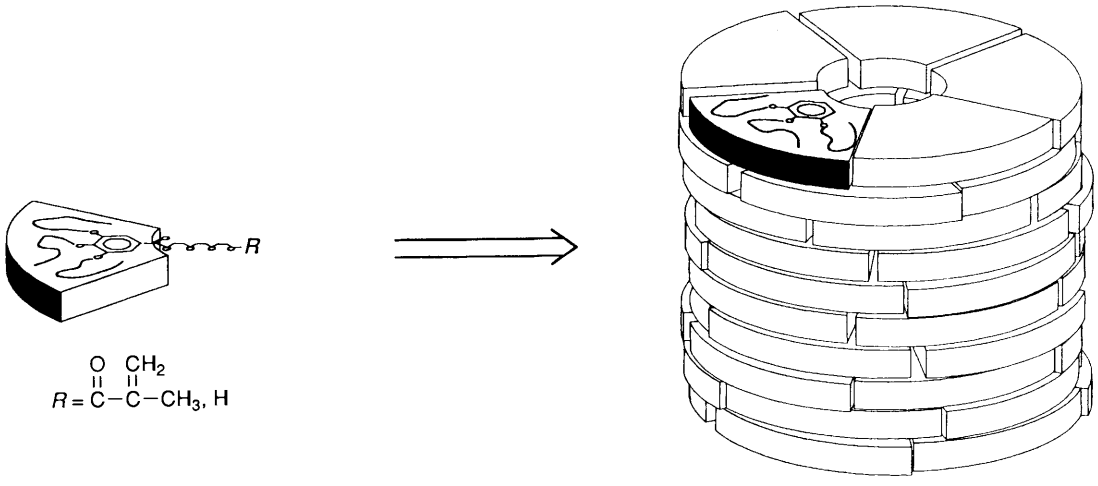

Fig. 9 Self-assembly of tapers into supramolecular cylindrically shaped architectures *via* 'molecular' and 'supramolecular' polymer backbones

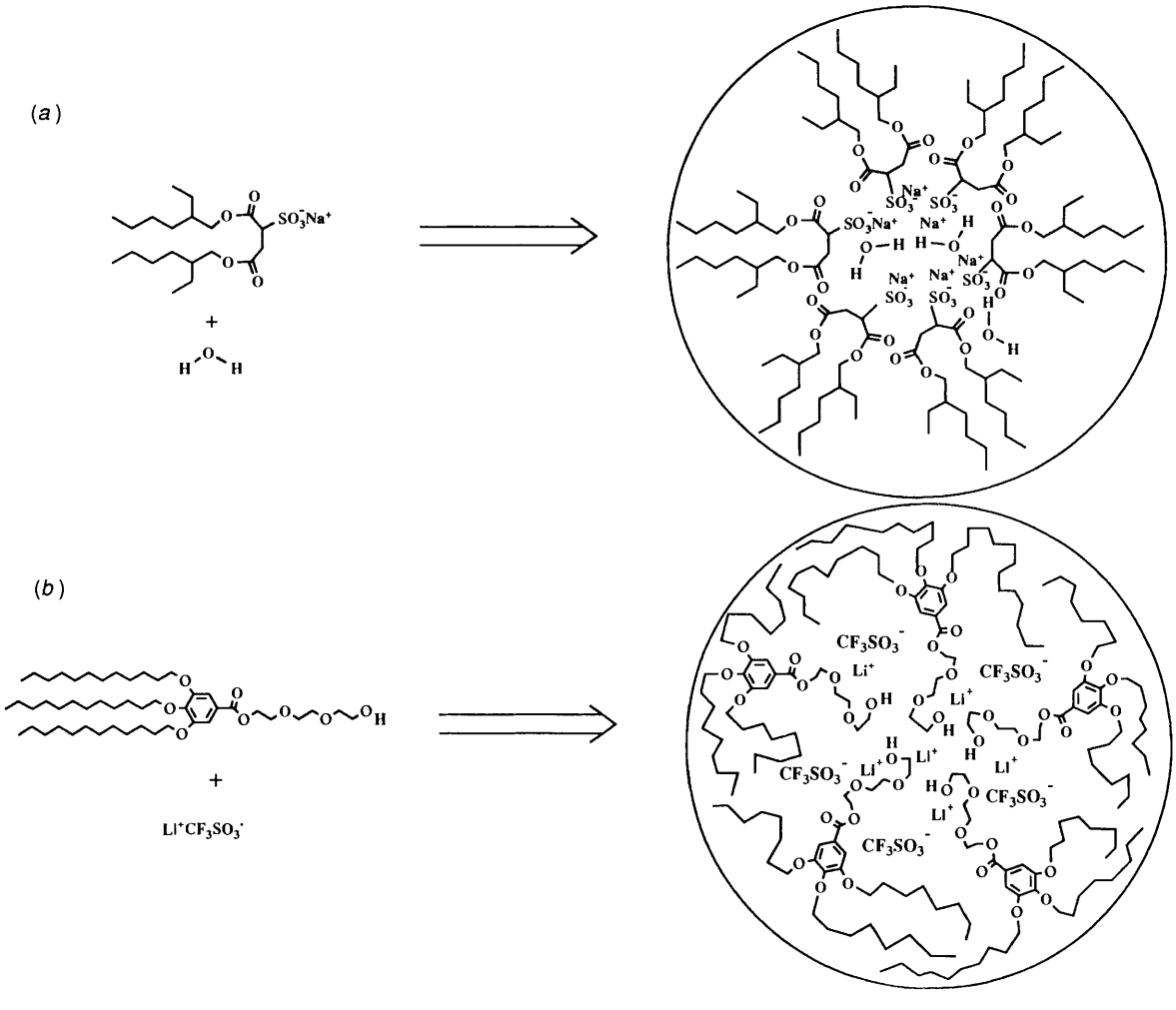

Fig. 10 (*a*) The formation of a cylindrical inverse micelle by the sodium salt of dioctyl sulfosuccinate (AOT) in water; (*b*) the formation of the cylindrically shaped architecture by **3-12-3** with $LiCF_3SO_3$

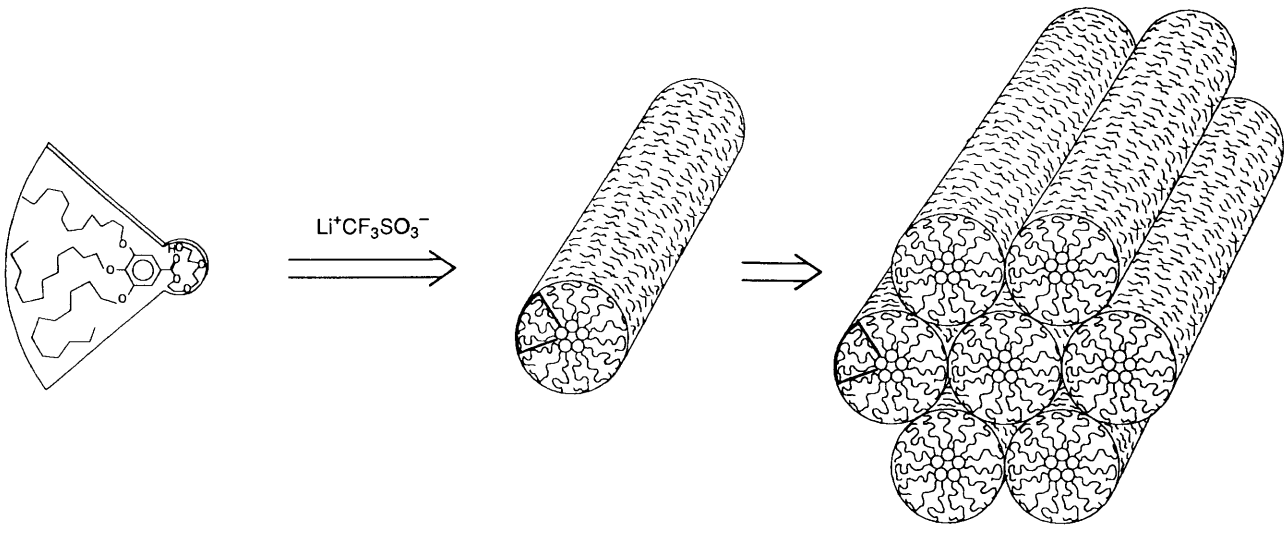

Fig. 11 The self-assembly of **3-12-3** with $LiCF_3SO_3$ into a cylindrically shaped inverse micelle and the packing of the columns into the hexagonal arrangement of the Φ_h mesophase

complexation by **3-12-3** and **3-18-3**, or from the formation of a covalent molecular backbone in **5-12-*n***. This self-assembled architecture represents the thermotropic analogue of cylindrically shaped inverse micelles which form lyotropic liquid crystalline phases.[5c] The resemblance between the two systems is illustrated in Figs. 10(*a*) and (*b*). The formation of an inverse micelle by the sodium salt of dioctyl sulfosuccinate (AOT)[14] in water is shown in Fig. 10(*a*). The formation of a cylindrically shaped architecture by **3-12-3** with $LiCF_3SO_3$ is shown in Fig. 10(*b*). Fig. 11 shows a representation of the self-assembly of **3-12-3** with $LiCF_3SO_3$ into a cylindrically shaped inverse micelle which packs into a hexagonal arrangement in the Φ_h mesophase.

Conclusions

Unlike the analogous DOBOB-based structures [Scheme 1(*a*)], the monoesters of OE endo-receptors with 3,4,5-tris(*n*-alkan-1-yloxy)benzoic acid [Scheme 1(*c*)] cannot self-assemble into a cylindrical architecture based solely on the strength of endo-recognition provided by H-bonding and dipolar interactions. This behaviour seems to result from the absence, in the latter compounds, of a pronounced taper shape (present in the DOBOB based structures) and therefore, of exo-recognition. However, the introduction of ionic interactions effected by the complexation of alkali-metal ions by the OE endo-receptor provides the endo-recognition necessary to compensate for the reduced taper shape and facilitate the self-assembly of **3-12-3** and **3-18-3** into a cylindrical supramolecular architecture which displays a Φ_h mesophase. Once the endo-recognition is enhanced by complexation, the self-assembly into the cylindrical architecture becomes highly dependent on the strength of exo-recognition. This is illustrated in the phase behaviour of $LiCF_3SO_3$ complexes of **3-7-3**, **3-12-3** and **3-18-3** in which the aliphatic content in the exo-receptor controls the thermal stability of the cylindrical architecture. The tendency towards self-assembly of the polymers **5-7-3**, **5-12-*n***, **5-12-*p*** and **5-18-3** is similarly highly dependent on the extent of endo- and exo-recognition. Replacement of the flexible OE spacer with a paraffinic spacer of the same number of atoms in length, also suppresses the formation of both Φ_h and crystalline phases. This result highlights the importance of the endo-recognition process for the self-assembly of the cylinders. The $LiCF_3SO_3$ complexes of **3-12-3** and **3-18-3**, as well as the polymers **5-12-*n*** represent an approach to the self-assembly of tubular architectures in which there is a delicate balance of the recognition processes. The T_i of the polymers show very little dependence on the length of the OE spacer. Decreasing the spacer length slows down the formation of the Φ_h mesophase which is well established for side-chain liquid-crystalline polymers.[15] The low molar mass compounds **3-12-3** and **3-18-3** are able to complex higher concentrations of $LiCF_3SO_3$ than the polymers **5-12-*n***. The self-assembling systems presented here are complementary to other systems which are under active investigation in other laboratories.[4b,c,16]

Acknowledgements

Financial support from the National Science Foundation (DMR-92-06781), and a NATO travelling grant are gratefully acknowledged. We also thank Professor S. Z. D. Cheng of the Department of Polymer Science of the University of Akron for the density measurements.

References

1 V. Percec, J. Heck, M. Lee, G. Ungar and A. Alvarez-Castillo, *J. Mater. Chem.*, 1992, **2**, 1033.
2 V. Percec, G. Johansson, J. Heck, G. Ungar and S. V. Batty, *J. Chem. Soc., Perkin Trans. 1*, 1993, 1411.
3 V. Percec, J. Heck, D. Tomazos, F. Falkenberg, H. Blackwell and G. Ungar, *J. Chem. Soc., Perkin Trans. 1*, submitted.
4 (*a*) A. Klug, *Angew. Chem., Int. Ed. Engl.*, 1983, **22**, 565; (*b*) J. S. Lindsey, *New J. Chem.*, 1991, 153; (*c*) G. M. Whitesides, J. P. Mathias and C. T. Seto, *Science*, 1991, **254**, 1312.
5 (*a*) J. N. Israelachvili, *Intermolecular and Surface Forces*, 2nd edn., Academic Press, New York, 1991; (*b*) A. Skoulios and D. Guillon, *Mol. Cryst., Liq. Cryst.*, 1988, **165**, 317; (*c*) H. Finkelmann and E. Jahns, *Association and Liquid Crystalline Phases of Polymers in Solution*, in *Polymer Association Structures: Microemulsions and Liquid Crystals*, ed. M. A. El-Nokaly, *ACS Symp. Ser.*, 1988, **384**, p. 1; (*d*) H. Ringsdrof, B. Schlarb and J. Venzmer, *Angew. Chem., Int. Ed. Engl.*, 1988, **27**, 113; (*e*) J. Charvolin and A. Tardieu, *Lyotropic Liquid Crystals: Structure and Molecular Motions*, in *Liquid Crystals*, ed. L. Liebert, Academic Press, New York, 1978, p. 209.
6 J. Malthete, A. Collet and A. M. Levelut, *Liq. Cryst.*, 1992, **11**, 93.
7 V. Percec and J. Heck, *Polym. Bull.*, 1991, **25**, 431.
8 V. Percec, J. Heck, D. Tomazos and G. Ungar, *J. Chem. Soc., Perkin Trans. 2*, in the press.
9 A. Keller, G. Ungar and V. Percec, *Liquid Crystal Polymers: A Unifying Thermodynamics Based Scheme*, in *Advances in Liquid Crystalline Polymers*, eds. R. A. Weiss and C. K. Ober, *ACS Symp. Ser.*, 1990, **435**, 308.
10 (*a*) P. S. Pershan, *Structure of Liquid Crystal Phases*, World

Scientific, Singapore, 1988; (*b*) W. Helfrich, *J. Phys. Colloq., C3*, 1979, **40**, 3; (*c*) V. Percec, J. Heck and G. Ungar, *Macromolecules*, 1991, **24**, 4957.
11 G. Ungar, *Polymer*, 1993, **34**, 2050.
12 C. R. Safinua, K. S. Liang, W. A. Varady, N. A. Clark and G. Anderson, *Phys. Rev. Lett.*, 1983, **53**, 1172.
13 V. Degiorgio and M. Corti (eds.), *Physics of Amphiphiles: Micelles, Vesicles and Microemulsions*, North-Holland, Amsterdam, 1985.
14 (*a*) P. Ekwall, L. Mandell and K. Fontell, *J. Colloid Interface Sci.*, 1970, **33**, 215; (*b*) E. I. Frances and T. J. Hart, *J. Colloid Interface Sci.*, 1983, **94**, 1.
15 (*a*) V. Percec and C. Pugh, *Molecular Engineering of Predominantly Hydrocarbon Based Liquid Crystalline Polymers* in *Side Chain Liquid Crystalline Polymers*, ed. C. B. McArdle, Blackie, Glasgow and Chapman and Hall, New York, 1989, p. 30; (*b*) V. Percec and D. Tomazos, *Molecular Engineering of Liquid Crystalline Polymers*, in *Comprehensive Polymer Science*, First Supplement, ed. G. Allen, Chapman and Hall, New York, 1989, p. 30; (*b*) V. Percec and D. Tomazos, *Molecular Engineering of Liquid Crystalline Polymers*, in *Comprehensive Polymer Science*, First Supplement, ed. G. Allen, Pergamon, Oxford, 1992, pp. 299–383; (*c*) V. Percec and D. Tomazos, *Adv. Mater.*, 1992, **4**, 548.
16 For a few representative reviews on self-assembly and self-synthesis see: (*a*) J.-M. Lehn, *Angew. Chem., Int. Ed. Engl.*, 1988, **27**, 89; *Angew. Chem., Int. Ed. Engl.*, 1990, **29**, 1304; *Makromol. Chem. Macromol. Symp.*, 1993, **69**, 1; (*b*) D. Philp and J. F. Stoddart, *Synlett*, 1991, 445; (*c*) J. F. Stoddart, Series ed., *Monographs in Supramolecular Chemistry*, RSC, Cambridge, UK; (*d*) G. W. Gokel ed., *Supramolecular Chemistry*, Vol. 1 (1990), Vol.2 (1992), JAL Press, Greenwich; (*e*) V. Balzani and L. De Cola, eds., *Supramolecular Chemistry*, Kluwer, Dordrecht, 1992; (*f*) E. Weber, ed., *Supramolecular Chemistry I-Directed Synthesis and Molecular Recognition* in *Top. Curr. Chem.*, vol. 164, 1993; (*g*) F. Vögtle, *Supramolecular Chemistry*, Wiley, New York, 1992.

Paper 3/04571D
Received 30*th July* 1993
Accepted 22*nd September* 1993